Secure and Optimized Data Sharing Model Group in Healthcare Cloud Environment

Uma Hombal, Dayananda R.B.

Abstract-The cloud computing provides convenient on-demand access of the data. Sharing of data in the cloud computing will enable several users to easily handle the data that is being shared. The medical-field finds more advantages by the cloud-computing technology as the data can be accessed anywhere and anytime by the patients as well as this data can be shared with other medical-practitioners. This alarms for the security issues as the huge amount of sensitive data is being shared. The data must not be available to malicious-attackers. In this paper, we propose the block-design based key agreement protocol in order to share the data securely and the design provides fault-detection and fault-tolerance. The group-data model PSM is given with the block-based design, which decides how the sharing of the data is done by grouping and giving positions to users in particular blocks and the column. The $(np, i + 1, 1)$ design is proposed in our paper, which gives the technique for positioning of the users. The encryption and decryption of data is done and their times cost according to file size is found. The comparison of the time-cost for our model and existing models is compared with respect to different number of simulations.

Keywords: Cloud-computing, data-sharing, block-based design, group-key

I. INTRODUCTION

Health-care requires continuous innovations in all the fields in a systematic way in order to provide high quality services. Technology of Information is rapidly and vastly used in healthcare with the motivation of to enhancing and improvising the medical services for cost reduction. Modern health-care innovations rely on information system in all aspects. The application of information-technology in health-care has got its importance in all the countries [1]. Most of the services that are provided are being outsourced to the cloud servers. The cloud storage plays a very important role in the applications like the medical files transferring etc. The majority of data being outsourced will be the health-care data, which will include the personal health record, Electronic health record and related documents. The patients are sent to various tests which results in high exchange of data between different departments of medical units. But this must be done in a secure manner. Many researches have been done to protect the data that is being shared between different departments of these medical units and to identify the risks in sharing of this data [2] [3] [4].

The technology used which helps in this data-exchange is cloud computing. Cloud computing is said to be a model that enable on demand service. The resources can be dynamically increased which implies lot of medical data can be stored and this data can be used and can be accessed anywhere and anytime by the patients or the doctors as well as share the information among them.

This alarms for the security and privacy issues as large amount of sensitive data will be shared. The patients' data must not be accessible to malicious attackers. The compromise in this data will be a threat to both the patient and the organization with whom the patient exchanges the data. Methods are taken to provide this security against the attacks [5]

Considering this application of information technology in health-care, the personal health record being outsourced to the servers has gotten numerous data-breaches related to cloud servers which includes the malicious attacks. Patients are unable to have any physical control over their own health-record. These sensitive data are not under the control of the control of these data-owners. So there requires an encryption mechanism to protect these records before out-sourcing is done. Here the owner must decide which user will get access to which data in this record. The decryption mechanism must be such that only those with the decryption ley must be able to decrypt and obtain the data [6] [7]. This implies that the authoritative-users get the access to the data that is being shared outsourced to the cloud.

In this paper we concentrate the sharing of data to multiple users. Here the multiple users will form a group and thereby exchange the data. Here the block-based design key-agreement way is used to design the block-based design structure which can support multiple-participants. This design helps all the data holders to share their data with the higher security as well as a much more efficient manner. This presents the group data-sharing model that supports sharing of this health-care data in a group manner. This DS(data sharing) model in group provides the definition of block based design which is symmetric which determines the way communication among the groups take place. It brings the concept of group-key that the multiple participants generate to share data in a secure manner. The group members make key-agreement to derive the common group-key. This key is being generated by the users themselves. Due to this, any sorts of attacks to the key is avoided and thereby the attack on the data is avoidable. The fault-detection and fault-tolerance is provided by this design. This ensures the group-key is being generated without failure. The fault-detection is done. In this, it can identify the volunteer who can replace the malicious-attacker. This enables to avoid different key-attacks which once again makes data sharing safe. In this, the CCSTPV i.e. the cloud-security service third-party-verifier is used. This is useful in providing the key-updates. It helps the user, to encrypt the file by using the key provided by the CCSTPV and thereby outsource the data to cloud, this encryption makes the data secure for against any middle-attacks.

This paper has organized in subsequent sections that are as follows, section- 2 discuss the Literature survey, in section 3 we described proposed model, section-4 we provide the result-analysis, section-5 gives the conclusion of our paper.

Retrieval Number: A4602119119/2019©BEIESP
DOI: 10.35940/ijitee.A4602.119119

5320

Published By:
Blue Eyes Intelligence Engineering
& Sciences Publication

Multi-tier Framework for Optimizing Pairwise Key Predistribution in Sensory Applications

Vaneeta M, S. Swapna Kumar

Abstract: *Security has been always a prominent concern in Wireless Sensor Network (WSN) irrespective of the evolution of various scientific approaches that mainly mechanizes key management approaches to secure the communication system among the resource constraints sensors. Out of various key management approaches, pairwise key is one effective approach to ensure cost effective key management scheme; however, review of existing approaches shows that they still are characterized by various issues connected to optimized performance. Adopting analytical research methodology, the proposed system implements an optimized multi-tier framework for resisting key-based threats and it targets to introduce a lightweight pair wise predistribution of keys by joint integration of enhanced public key encryption and digital signature. The study outcome shows that proposed system offer a better security performance in contrast to existing pair wise predistribution of keys.*

Keywords: *Pairwise keys, predistribution, Key agreement, Security, Attacks.*

I. INTRODUCTION

The adoption of the Wireless Sensor Network (WSN) has been prominently increasing owing to its cost effective remote monitoring capabilities [1],[2]. The sensors follow various clustering schemes in order to carry out data aggregation process [3],[4]. In such communication scheme, usually the members nodes forward the physically sensed data to their assigned cluster head which is then forwarded to either sink (using single hop) or to different cluster head (using multihop). Although, WSN is completely backed up by a stable topology as well as infrastructure, but there are always good possibilities of faults among the operations being carried out by the resource constrained sensor. There are various possibilities of intrusion in WSN both in the form of internal or external attack. There are various studies that have been discussed for addressing key agreement issue with respect to self-enforcing approach, trusted-server approach, and key predistribution approach [5],[6]. Out of all these, key predistribution scheme is found to be more used in existing system that distributes the information of secret keys is carried out before the sensors are actually deployed in the simulation. The decision of the keys can be well defined in advanced if the neighborhood information exists, which is

quite impractical as majority of the deployment strategy of the sensors are actually randomized and not on predefined basis. At present, there are various predistribution schemes in WSN that doesn't use such dependency of apriori information of the deployment of sensors. The better form of the solution will be to allow the complete set of the sensors to use a secret key that can be considered as master key. In order to achieve a better form of key-agreement, it is now feasible for different sensors to utilize this master secret key and thereby get the pairwise secret key [7]. However, such approaches are found to reduce the resiliency of the WSN performance that is not anticipated. It will mean that upon event of a compromisation of even a single sensor than the complete network will be rendered vulnerable.

Existing mechanism from the literatures recommends reposting such master key over certain form of hardware that is free from any form of physical damage or any security risk [8],[9]. It will mean that hardware-based approach is claimed to offer protection towards such master key; however it is not completely feasible as it will maximize the consumption of resources as well as cost associated with each sensor. At the same time, there is no evidence till date that hardware based security approaches are always safe as there is the possibility to break-in. There are certain other forms of the predistribution scheme of the secret keys in WSN that allows the sensors to carry a specific number of secret keys in the form of pairwise and this information is accessible only for that specific sensor node while the another specific sensor node in the form of source and destination respectively. It is claimed that such security policies are potentially strong as it is not feasible for the adversary node to influence the security strength of other sensors. Unfortunately, such approaches are not considered as practical approaches as they cannot be supported by sensors with restricted memory.

Another significant problem is that it is not feasible for adding new sensors as there is no new secret key to be allocated by the existing deployed sensors. Therefore, the proposed system discusses about a novel approach of pairwise key distribution scheme where applicability of the different test environment is valid. The idea is to ensure multi-tier framework by including a superior authentication scheme using enhanced public key encryption and digital signature. The prime agenda of the work is also to resist various forms of malicious attacks of dynamic order. The organization of the paper is as follows: Section "A" discusses about the existing literatures where different techniques are discussed for detection schemes used in power transmission lines followed by discussion of research problems in Section

Integrated System for Classification of Pulmonary Nodules on CT Images

Vijayalaxmi Mekali, Girijamma H. A

Abstract: Mortality rate of lung cancer is increasing very day all over the world. Early stage lung nodules detection and proper treatment is solution to reduce the deaths due to lung cancer. In this research work proposed integrated CADe/CADx system segments and classifies lung nodules into benign or malignant. CADe phase segments Well Circumscribed Nodules (WCN), Juxta Vascular Nodules (JVN) and Juxta Pleural Nodules (JPN) of different size in diameter. This part uses algorithms proposed in our previous WCN, JVN and JPN lung nodules segmentation work. CADx performance classification of segmented WCNs, JVNs and JPNs nodules into benign or malignant. In first part of CADx system hybrid features of segmented lung nodules are extracted and features dimension vector is reduced with Linear Discrimination Analysis. Finally, Probabilistic Neural Network uses reduced hybrid features of segmented nodules to classify segmented nodules as benign or malignant. Proposed integrated system achieved high classification accuracy of 94.85 for WCNs, 97.65 for JVNs and 97.96 for JPNs of different size in diameter (nodules diameter< 10mm, nodules diameter >10mm and < 30mm, nodules diameter >30mm and <70mm). For small nodules achieved classification performance values are, accuracy of 94.85, sensitivity of 90 and specificity of 95.85. And nodules of size 10mm to 30mm obtained accuracy, sensitivity and specificity are 97.85, 97.65 and 94.15 respectively.

Keywords : Computer Aided Detection/Diagnosis, Lung nodules, Low Dose Computed Tomography, PNN.

I. INTRODUCTION

Lung cancer is most dangerous disease with high death rate. According to 2018 lung cancer survey by World Health Organization (WHO), lung cancer new cases have risen to 2.09 million and 1.76 million deaths all over the world. Early stage detection of lung cancer is one possible and acceptable solution to reduce the death rate [17]. Lung cancer is complex disease which can be classified into different type according its site of origin, cells size, and attachment of external structures, malignancy rate and solidity. Well Circumscribed Nodules (WCN) are round or oval shaped lung nodules appears in center of lung area without any additional tissues attachment. Juxta Vascular Nodules (JVN) are attached with blood vessels and Juxta Pleural Nodules (JPN) are attached with lung pleural. At next level WCNs, JVNs and JPNs are classified into solid, part-solid and non-solid nodules. Based on severity, lung nodules are either benign or malignant.

Small nodules without cancerous cells are known as benign nodules. Moderate or large size nodules with cancerous cells are known as malignant (have potential to spread to other sites) [18]. Malignancy of malignant lung nodules indicates potential of these nodules to extent to lymph nodes, or another lung lobe or other organs like breast, brain, prostate etc. Farthest speared of malignant nodules indicates higher malignancy. Table I provides characteristics of benign and malignant nodules.

A. Low Dose Computed Tomography (LDCT) and Computer Aided Detection/Diagnosis (CADe/x) system for lung cancer

Among all the imaging modalities LDCT is GOLD STANDARD for detection of lung cancer [17]. As LDCT generates multiple CT images (slices) in one scan, interpretation of such huge number of slices by radiologist to extract the information of existence nodules is challenging task. Thus, now a days cancer detection/diagnosis medical routines uses CADe/x system to get precise information about nodules. CADe system assist the radiologist in detection of nodules and benign or malignant nodules classification is done by CADx system and it thus helps the radiologist in treatment plan. Fig. 1 is CT lung image showing different anatomical structures of lung and red circle shows the presence of lung nodule.
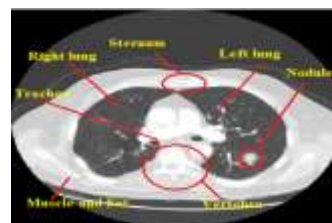

Fig. 1.Lung CT image with different parts and lung nodule.

Table-I: Characteristics of benign and malignant nodules

Characteristics	Benign	Malignant
Shape	Round or Oval	Irregular
Boundary Smoothness	Smooth	Irregular
Size	Less than 3cm in diameter	Greater than 3cm in diameter
Indication of cancer	Non-cancerous	Cancerous
Malignancy	No or very poor	High

Vijayalaxmi Mekali, Department of Computer Science and Engineering, Kammavari Sangham Institute of Technology, Visvesvaraya Technological University, Bangalore, India. Email: duruth.viju@gmail.com

Dr. Girijamma H. A, Professor, Department of Computer Science and Engineering, R. N. S Institute of Technology, Visvesvaraya Technological University, Bangalore, India.. Email: girijakasal@gmail.com

Novel CADe/CADx System for Lung Nodules Segmentation and Classification on Computed Tomography Images

Vijayalaxmi Mekali, Girijamma H. A

Abstract: *Detection and classification of different types lung nodules poses major challenges in medical diagnosis routine. Classification of segmented nodules based on extracted hybrid features of segmented nodules have shown remarkable performance. Recently deep features alone and also with combination of hybrid features have improved nodules classification. In this research work new CADe/CADx system is proposed for detection and classification of Well Circumscribed Nodules, Juxta Vascular Nodules and Juxta Pleural Nodules. In nodules detection part, algorithms proposed in our previous work were used. Classifiers decision fusion based new nodules classification system is proposed. Four set of hybrid features and deep features using Convolution Neural Network are considered from segmented nodules. Hybrid features set consist of twenty four shape features, six GLCM features in four direction with a distance of two, six First Order Statistic features and twelve energy features. Five individually trained Probabilistic Neural Networks by all five set features separately used in nodule classification. In classification process all five classifiers decisions are fused at 2-level, 3-level, 4-level and 5-level. The proposed system achieved highest performance with 5-level fusion compared with other level fusions. System was evaluated on CT images of LIDC database with consideration of 2669 lung nodules of malignancy rate 1 to 5. Based on malignancy rate 2669 nodules are grouped as dataset 1 and dataset 2 with nodules of malignancy rate 1, 2, 3 and 3, 4,5 respectively. The 5-level decision fusion achieved highest accuracy of 95.72, sensitivity of 95.52, specificity of 95.79 and Area Under Curve of 96.21 for dataset 1 and accuracy of 92.54, sensitivity of 90.48, specificity of 94.63 and Area Under Curve of 92.69 for dataset 2.*

Keywords: **Computed Tomography, Computer Aided Detection/Diagnosis, Convolution Neural Network, Lung cancer and Lung Nodule Classification.**

I. INTRODUCTION

All over the globe mortality rate of lung cancer is very high as compared with other types of cancers such as prostate, brain, breast, cervical cancer. According to World Lung Cancer Day 2019 facts and figure, lung cancer new cases have risen to 2.09 million and 1.76 million deaths all over the world. Early stage detection and classification of lung cancer is acceptable solution to reduce the mortality rate. Lung cancer is heterogeneous disease as it appears at different

Vijayalaxmi Mekali*, Department of Computer Science and Engineering, Kammavari Sangham Institute of Technology, Visvesvaraya Technological University, Bangalore, India. Email: duruth.viju@gmail.com
Dr. Girijamma H. A, Department of Computer Science and Engineering, R. N. S Institute of Technology, Visvesvaraya Technological University, Bangalore, India.. Email: girijakasal@gmail.com

locations in lungs attached with different types of external structures with different calcification rate. Lung cancer can be classified into different type according its site of origin, cells size, and attachment of external structures, malignancy rate and solidity. Well Circumscribed Nodule (WCN) is round or oval shaped lung nodules appears in center of lung area without any additional tissues attachment. Juxta Vascular Nodule (JVN) is attached with blood vessels and Juxta Pleural Nodule (JPN) attached with lung pleural as shown in Fig. 1. At next level WCNs, JVNs and JPNs are classified into solid, part-solid and non-solid nodules. Based on severity lung nodules are either benign or malignant. Small nodules without cancerous cells are known as benign nodules. Moderate or large size nodules with cancerous cells are known as malignant (have potential to spread to other sites). Malignancy of malignant lung nodules indicates potential of these nodules to extent to lymph nodes, or to another lung lobe or to other organs like breast, brain, prostate etc. Farthest speared of malignant nodules indicates higher malignancy. Table I shows the characteristics of benign and malignant nodules.

A. Low Dose Computed Tomography (LDCT) and Computer Aided Detection/Diagnosis (CADe/x) system for lung cancer

Medical modalities like X-ray, Computed Tomography (CT), Magnetic Resonance Imaging (MRI), Positron Emission Tomography (PET) and Diffusion Weighted-MRI (DW-MRI) have been playing major role in detection of lung cancer. Among all the medical modalities Low Dose CT (LDCT) is GOLD STANDARD for detection of lung cancer. LDCT generates huge number of images (slices) in one single scans. It is tedious task for radiologist to interpret all the slices to draw useful information about existing nodules. To reduce the burden of radiologist and for accurate detection of lung cancer nodules, medical routines uses Computer Aided Detection/Diagnosis (CADe/x) system to detect and draw precise information about nodules. Benign or malignant nodules classification is done by CADx system and thus it helps the radiologist in treatment plan.

B. Role of Image processing techniques and classifier in lung cancer diagnosis

Image processing techniques such as different types of thresholding methods, Region Growing (RG) method, clustering algorithms, morphological operations, edge

165

A Survey on Motion Detection by Image Stitching techniques

Kashika P H
Research Scholar, CSE Dept
Visvesvaraya Technological University
Regional Centre, Kalaburagi

Rekha B Venkatapur
Professor, HOD, CSE Dept
KSIT College of Engineering
Bengaluru

Jayashree Agarkhed
Professor, CSE Dept
PDA College of Engg
Kalaburagi

Abstract: In today's world, an image stitching/homogenizing is considered as a dynamic research area in graphics and computer vision. Image homogenizing literature shows that it is a challenging task for panoramic images. Panorama Image stitching is the process of merging two or more images of the same scene into one high resolution seamless image called as panoramic image. Tracking motion and moving object identification is the basic source to extract important information regarding moving objects from anomalous sequences in continuous image based surveillance systems. This paper presents a survey study about the process of panoramic image stitching(PIS) process and the main components of PIS. Further, a framework of a complete panorama image stitching system to detect the moving objects based on these approaches will be introduced.

Keywords- Image stitching; Panorama; object detection; Surveillance; seamless image

I. INTRODUCTION

Image/video stitching or photo homogenizing is the process of combining multiple photographic images with overlapping fields of view to produce high- resolution image/video or segmented panorama to track and detect the moving objects. Insurgent incidents like terrorist attacks or several others, abandoned objects were used to threaten the harmony of community and sovereignty in India. Many damages are caused due to such unusual incidents to public/private properties causing financial losses as well as pulled people in emotional trauma. One solution is to use public surveillance camera to detect anomalous events and trigger alarms to vigilance and authority. Most approaches to image stitching nearly require exact overlap between the identical exposures and the images to produce seamless results performed commonly through the use of computer software which is known as mosaicing. Algorithms for aligning images and stitching them into seamless photo-mosaics are most widely used in computer vision. Image stitching algorithms create the high resolution photo-mosaics used to detect today's digital maps and satellite photos. They also come bundled with most digital cameras currently being sold, and can be used to create beautiful ultra wide-view panoramas. The aim of this project is to create software that merge images which have similar features and create a panoramic image for moving object detection using surveillance cameras. Recognition/identification of the object and its motion/activities with least amount of processing is required which is compromised in research area whenever high accuracy is met.

II. LITERATURE SURVEY

Over the period of last many years, several approaches have been proposed for image stitching and motion detection. Image stitching is a process in which several images are stitched together after establishing geometric relationship between them. The geometric relationships are coordinate transformations that relates usually the various coordinate systems. By applying these transformations via a merging operation and by combining the overlapping of the images it is possible to create a noteworthy form of mosaic.

The two main expectations from the image homogenizing process are that the Stitched image should be nearly as close as possible to input images and in Stitched images the seams should be invisible. New algorithms are coming to make the work clear and less tedious for the programmers to work upon. In the era of 3-D imaging and videos, image/video stitching is an inevitable task. Hence, there is a large scope for research in this field.

The authors in paper[1], presented a real-time video stitching system which can stitch videos acquired from multiple moving cameras, so that cameras could move freely to stitch the videos. They proposed an algorithm which estimates refined homography in both spatial and temporal domains. That is, their work initially detects feature points by SURF and then by K-Nearest Neighbors (KNN) method, they accomplished feature matching. Further, subsequently they applied RANSAC to estimate homography transformation from the extracted feature pairs in the spatial domain. In experimental setup, they stitched three videos acquired from three cameras placed on a linear

A SURVEY ON APPLICATION OF DEEP LEARNING: UNSUPERVISED AUTO ENCODER

Mr.Raghavendrachar S[1] , Dr. Rekha B Venkatapur[2]

[1]*Assistant professor, Department of Computer Science and Engineering, KSIT, Bengaluru-560109,*

[2]*Professor & Head, Department of Computer Science and Engineering, KSIT, Bengaluru-560109,*

Abstract – Deep Learning is playing an increasingly important role in our lives. Deep learning is not a restricted learning approach, but it abides various procedures and topographies which can be applied to an immense speculum of complicated problems. Deep learning methods have made a significant break-through with appreciable performance in a wide variety of applications with useful security tools. It is considered to be the best choice for discovering complex architecture in high-dimensional data by employing back propagation algorithm. Deep learning has already made a huge impact in areas, such as cancer diagnosis, precision medicine, self-driving cars, predictive forecasting, biological image classification, speech recognition, smart city and many more. This paper mainly focuses on the working of unsupervised auto encoders and its applications.

*KeyWords***:** Deep Learning, back propagation, unsupervised learning, auto encoders,

I. INTRODUCTION

Machine learning is a subsection of Artificial Intelligence that imparts the system, the benefits to automatically learn from the concepts and knowledge without being explicitly programmed. Neural Network is a machine learning technique that is inspired by and resembles the human nervous system and the structure of the brain. It consists of processing units organized in input, hidden and output layers. The nodes or units in each layer are connected to nodes in adjacent layers. Each connection has a weight value. The inputs are multiplied by the respective weights and summed at each unit. The sum then undergoes a transformation based on the activation function, which is in most cases is a sigmoid function, tan hyperbolic or rectified linear unit (ReLU).The implementation of neural networks consists of the following steps:

1. Acquire training and testing data set
2. Train the network
3. Make prediction with test data

Deep learning technology works on the Artificial Neural Network system (ANNs). These ANNs constantly take learning algorithms and by continuously increasing the amounts of data, the efficiency of training processes can be improved. Deep learning is also known as deep structured learning and hierarchical learning that consists of multiple layers which includes nonlinear processing units for the purpose of conversion and feature extraction.

In the Deep learning methodology, the term "Deep" enumerates the concept of numerous layers through which the data is transformed. It must be noted that there is a difference between Deep learning and Representational learning. Representational learning includes

Taylor & Francis
Taylor & Francis Group

Shop floor to cloud connect for live monitoring the production data of CNC machines

Prathima B A, Sudha P N & Suresh P M

Published online: 28 Jan 2020.

Submit your article to this journal ⬈

View related articles ⬈

View Crossmark data ⬈

HOSTED BY

ELSEVIER

JESTECH

Full Length Article

Power optimization in MANET using topology management

Check for updates

B. Devika *, P.N. Sudha

Kammavari Sangham Institute of Technology, India

ARTICLE INFO

ABSTRACT

Mobile ad-hoc network (MANET) is a wireless ad hoc network, which is quickly deployable and functions without any infrastructure. This work proposes a hybrid optimization algorithm, named Chronological-Earth Worm optimization Algorithm (C-EWA), for performing effective clustering and adjusts power and energy parameters using topology management. In this paper, initially a graph that is equivalent to the network is constructed, and then, clustering of the graph is performed using the proposed C-EWA to generate an optimal cluster head. C-EWA is developed by the integration of chronological theory in EWA, with the use of the objective function. Here, the objective function considers several factors that involve power, connectivity, mobility, link lifetime, and distance. After choosing appropriate clusters, each of the nodes that belong to the cluster constructs a Gabriel graph within the corresponding cluster. Once the Gabriel graph is constructed, each node updates the list of neighbor and maintains the graph connectivity and adjusts the power of transmission based on the connectivity. The performance of the proposed method shows superior performance in terms of remaining battery power, mobility, throughput, delay and connectivity with values of 21.960 J, 0.729, 0.713, 0.295, and 5.256, respectively.

1. Introduction

Mobile Ad-hoc Network (MANET) is an autonomous wireless ad hoc network that contains mobile nodes, which initiate transmission without considering base stations [1]. Networking is essential for the strategic networks, which are not depended on other infrastructures that involve disaster relief organizations and military [2]. Several challenges related to network protocols are presented in MANET [3]. The protocols should offer distributed solutions whenever the centralized control and the access points are absent. The node mobility is inessential as compared to routing protocols [4], which can track the topology of the network [5]. The surplus of routing protocols deployed for MANETs perform certain tasks for data transmission. The changing topologies, network division, bandwidth, larger error rates, interference, power constraints, and collision are the issues in the network control for designing larger level protocols that involve routing and executing applications using the Quality of service (QoS) [6].

The MANET is adapted in several applications that range from the battlefield to the user's living room. Due to the limited battery energy of mobile nodes, how to prolong the lifetime of nodes and network becomes the key challenge in MANET, and it has received more and more attentions. The traditional methods employed for conserving energy are the spotlights on controlling transmission power and the dynamic turning of active nodes in the network. The reduction of energy utilization is controlled by transmission power, which subsequently results in effective data transmission and prolonging network lifetime [7]. Power plays a vital role in MANET [8,9] and requires fewer infrastructures and communication networks. The routing becomes challenging due to varying topologies produced by the movement of the node, and thus, the routing is a center of attraction among researchers. The existing routing protocols, like Ad hoc On-Demand Distance Vector (AODV) [10], Temporally Ordered Routing Algorithm (TORA), and Dynamic Source Routing (DSR), do not fulfill the requirements of real time applications. The application requires the communication network to provide a guarantee regarding QoS parameters. The prolonged battery life is important due to the mobile nodes. The power received is an important parameter for initiating the communication in MANET [11].

The MANET nodes move freely from one place to another in a random manner. The topology of the network is changed unpredictably and rapidly. The nodes inside the transmission range can directly exchange information with each other. The nodes that reside outside the transmission range should communicate indirectly by adapting the multi-hop routing protocol. Each node is responsible for the route discovery in a dynamic manner. Despite several clustering schemes, the organization of MANET into a

* Corresponding author.
    E-mail address: devikabgowda@gmail.com (B. Devika).
    Peer review under responsibility of Karabuk University.

Edge Detection and Contour Based Ear Recognition Scheme

Deven Trivedi, G. H. Patel College of Engineering and Technology, Anand, India

Rohit Thanki, C. U. Shah University, Wadhwan, India

https://orcid.org/0000-0002-0645-6266

Surekha Borra, K. S. Institute of Technology, Bengaluru, India

ABSTRACT

In recent days, with the advancements in computer vision technology pattern recognition for biometric data has been the focus of many researchers. The human ear can be used to assist in the recognition of an individual. In this article, a new scheme for ear recognition is presented, based on edge features such as the helix shape and contours between the edge pixels. First, an ear image is detected from the acquired image using a snake model-based image segmentation technique, and then histogram equalization is applied to form an enhanced ear image. After that, an Infinite Symmetric Exponential Filter (ISEF) edge is applied to the image, the contouring of edges is calculated, and then the contour values of pixels are extracted as ear features. Finally, the ear matching is performed between query ear features and enrolled ear features. Based on the matching score, the decision about individual authentication is performed. The experimental results showed that this proposed scheme performs better than existing schemes in the literature.

KEYWORDS

Biometric, Canny, Contour, Ear, Edge, Shen-Castan

1. INTRODUCTION

Nowadays, an individual is recognized based on his/her biometric characteristics in many places like offices, institute, airports, etc. These biometric characteristics are divided into two types: physical and behavioral (Jain and Kumar, 2012; Jain and Nandakumar, 2012). The examples of physical characteristics of an individual are fingerprint, face, iris, palm print and ear. The examples of behavioral characteristics of an individual are speech, signature, and gait. The systems based on biometrics recognize an individual automatically using various computer vision and pattern recognition algorithms (Jain and Kumar, 2012; Jain and Nandakumar, 2012). The biometric systems are used mainly for two operations: verification and authentication. In these operations, the query biometric image is compared and matched with its closest image in the database. While the query image is compared with all the database images in case of authentication, it is compared with its enrolled image in case of verification.

Investigation of Mechanical properties of hybrid composites using Hemp and Aramid

Dr.Girish T.R.
Associate Professor
Dept of Mechanical Engg
KSIT , Bangalore

Dr. Keerthi Prasad.K.S
Professor
Dept of Mechanical Engg
VVIET , Mysore

Vinay. S
UG Student
Dept of Mechanical Engg
KSIT Bangalore

Mahesh.D
UG Student
Dept of Mechanical Engg
KSIT Bangalore

Abstract

In the recent years the development and characterization of reinforced polymer composite is more important in the field of advance materials. This paper focuses on the fabrication and characterization of hybrid composites using natural fibre like hemp with synthetic fibre like aramid with epoxy resin by hand layup technique. Aramid fibres are class of synthetic fibre with higher heat resistance and strong fibre, these are used in military and aerospace applications. Hemp fibres are extracted from stem of the hemp plant which have high strength to weight ratio, chemical treatment for hemp fibre has been carried out in order to reduce the moisture absorption by the fibres. Mechanical properties such as tensile, flexural and hardness for the developed hybrid composites has been found out. A comparative study has been carried out to analyze the strength of composite materials before and after chemical treatment of hemp fibres. It was observed that there is a slight improvement in the strength of composites developed chemically treated hemp fibres.

Key words : Hemp, Aramid, Hand lay up technique, chemical treatment.

1. Introduction

Composite materials are made of up two or more constituent material with different physical and chemical properties that when combined produce a material with unique characteristics. These material are stronger, lighter, or sometimes cheaper as compared with monolithic materials. Composite materials are generally used in bridges, structures, boat hulls, racing cars, storage tanks etc. The first level of classification is usually made with respect to the matrix constituent. The major composite classes include Organic Matrix Composites, Metal Matrix Composites and Ceramic Matrix Composites. The term organic matrix composite is generally assumed to include two classes of composites, namely Polymer Matrix Composites and carbon matrix composites commonly referred to as carbon-carbon composites. The second level of classification refers to the reinforcement form fibre reinforced composites, laminar composites and particulate composites. fibre Reinforced composites can be further divided into those containing discontinuous Fibre Reinforced Composites are composed of fibres embedded in matrix material. Such a composite is considered to be a discontinuous fibre or short fibre composite if its properties vary with fibre length. On the other hand, when the length of the fibre is such that any further increase in length does not further increase, the elastic modulus of the composite, the composite is considered to be continuous fibre reinforced. Fibres are the important class of reinforcements, as they satisfy the desired conditions and transfer strength to the matrix constituent influencing and enhancing their properties as desired. The orientation of the fibre in the matrix is an indication of the strength of the composite and the strength is greatest along the longitudinal directional of fibre. Today, there is renewed awareness for improving the properties of plastics based components to meet engineering requirements to compete with nano materials. Development of commercially viable green products such as wood plastic composites (WPC) based on natural sources for wide range of applications is increasing day by day**.** Lignocelluloses filled thermoplastic composite have been in use since 1980, wood plastic composites (WPC) share the major market. Various lignocelluloses materials such as jute, hemp, sisal, bagasse, coconut, banana, rice husk are in use. These are light in weight, non-toxic, and have lower abrasive properties. Synthetic fibres are also called man-made fibres, most of the time it is prepared by using petrochemicals. Fibres are obtained from artificial or man made sources, they consists of small unit or a polymer which is made out of many repeating units known as monomers. These include nylon, acrylics, polypropylene. These are produced in millions of tons all over the world.

2. Methodology

2.1. Materials

High performance epoxy resin LAPOX L12 with the curing agent K6 hardener manufactured by Atul industries Gujarat India were used as the matrix. Bi-directional Aramid fibre and Hemp fibres were used in making the hybrid composite material. The hybrid reinforced composite material has been fabricated with chemically treated hemp fibre by hand layup technique . The weight ratio of 10: 1 was maintained for epoxy and hardener, the specimens were prepared according to ASTM standards.

2.2 Chemical treatment of Hemp fibre

Natural fibres allow moisture absorption from the environment that causes poor bonding with the matrix materials due to the presence of cellulose, hemicelluloses, lignin, pectin. In order to over come this problem certain chemical treatment on the surface of the fibre is needed. I the present work the bi directional hemp fibre was treated with different percentage(5%, 10%) of Sodium hydroxide solution(NaOH) . As a result moisture absorption of the fibre will be reduced and increases the compatibility with polymer matrix.

2.3 Hand lay up technique

There are many techniques available in industries for manufacturing of composites such as vacuum bagging, resin transfer moulding etc. The hand lay-up process of manufacturing is one of the simplest and easiest methods for manufacturing composites, the process is shown in Fig 1. A primary advantage of the hand lay-up technique is to fabricate very large, complex parts with reduced manufacturing times.
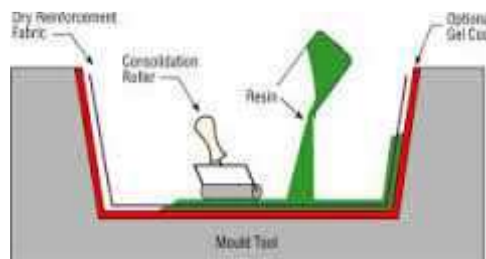

Fig 1: Hand lay up technique

2.4 Tensile Test

Tensile testing, also known as tension testing, is a fundamental materials science test in which a sample is subjected to a controlled tension until failure. Computerized Universal testing machine shown in Fig.2, which uses modern software for material test and analysis is used. . The Composite materials are usually gripped using some form of 'friction grip', where the load is transferred to the specimen through gripping faces which are roughened with serrations or a crosscut pattern.

Fig 2:Universal Testing Machine used for tensile test

2.5 Flexural Test

Flexural strength, also known as modulus of rupture, bend strength, or fracture strength a mechanical parameter for brittle material, is defined as a materials ability to resist deformation under load. The transverse bending test is most frequently employed, in which a specimen having either a circular or rectangular cross-section is bent until fracture or yielding using a three point flexural test technique. The flexural strength represents the highest stress experienced within the material at its moment of rupture.

Fig 3 Flexural test in Universal Testing Machine

2.6 Hardness test

The Rockwell scale is a hardness scale based on indentation hardness of a material. The Rockwell test determines the hardness by measuring the depth of penetration of an indenter under a large load compared to the penetration made by a preload. There are different scales, denoted by a single letter, that use different loads or indenters. The result is a dimensionless number noted as HRA, HRB, HRC, etc.,

Fig 4 Rockwell hardness testing machine

All experimental tests were carried out at Raghavendra Spectro Metallurgical Laboratory Bangalore India, tests were repeated three times to generate the data.

3   Results and Discussions

3.1 Tensile test

The tensile test was conducted for the developed composite material, specimens were prepared according to ASTM D638 standards. Sodium hydroxide(NaOH) solution(5% and 10%) is prepared by dissolving the NaOH pallets in the water. The bi directional hemp fibres are dipped in the prepared solution for 24 hours and dried in room temperature.
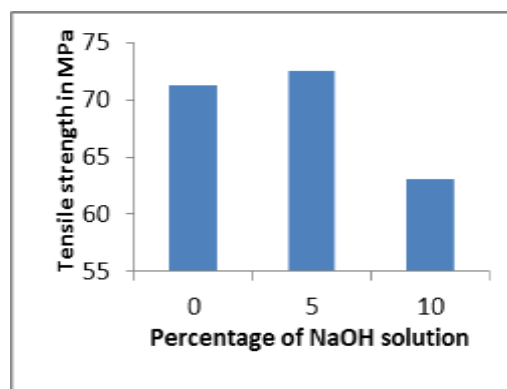

Fig 5 shows the tensile strength of hybrid composite

The chemical treatment enhances the binding strength between the fibre and the matrix also it is an effective way of cleaning the fibre surface and to increase the surface roughness. The tensile strength has increased for composites in which the hemp fibres are treated with 5% NaOH solution, further for 10% NaOH solution there is a slight decrease in the strength. Fig 5 shows the tensile strength of hybrid composite.

3.2 Flexural test

The flexural test has been carried out on the developed composite material, specimens were prepared according to ASTM D790 standards. Flexural test is conducted to measure the force required to bend the beam of a material to plastic limit also it is used to find the flexing stiffness of the material. Fig 6 shows flexural strength for hybrid composite materials.
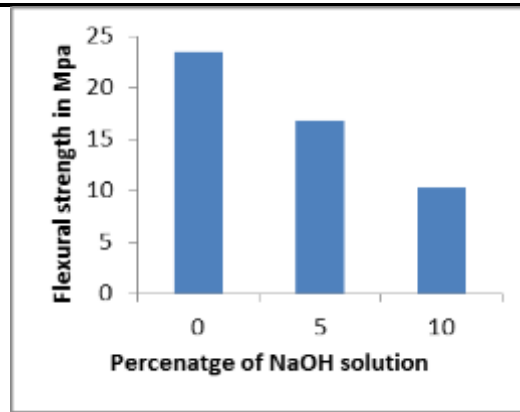
Fig 6 shows the flexural strength of hybrid composite material

3.3 Rockwell Hardness Test

In Rockwell hardness testing method the a preliminary test force is applied to the specimen using diamond ball indenter. This preload breaks through the surface to reduce the effect of surface finish. The depth of indenataion is measured by taking the preliminary test force for a specified dwell time. Fig 7 shows Rockwell hardness Number for hybrid composites.
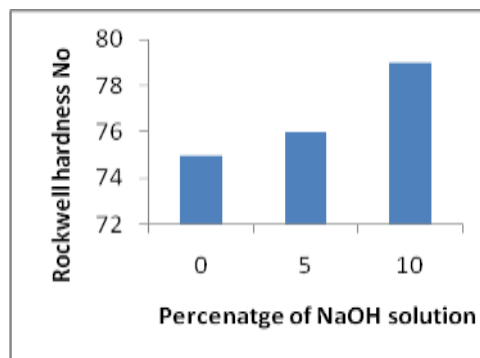

Fig 7 Shows the Rockwell hardness No for hybrid composite

4. Conclusions

The study on the effect of different fibre loading condition of Aramid/hemp fibre reinforced Epoxy based hybrid composites leads to the following conclusions:

1.The development of multi layered polymer hybrid composite using Aramid and chemically treated Hemp fibre with epoxy resin has been carried out successfully by hand layup technique.

2. The present investigation revealed that chemical treatment of hemp fibre has significant influence on the strength of the hybrid composite material. The maximum tensile strength was found to be 72MPa for composites prepared by 5% NaOH solution and there is a slight decrease in the strength for 10% NaOH solution.

3. The maximum flexural strength was found to be 24MPa for composites prepared by fibres which are not chemically treated.

4. The hardness of the hybrid composite material is increased as the percentage of NaOH is increased.

References

1   Asim Shahzad Hemp fibre and its composites - a review Journal of Composite Materials , http://jcm.sagepub.com/content/early/2011/08/04/0021998311413623.

2   N S Venkatesha Gupta Fabrication and evaluation of mechanical properties of alkaline treated sisal/hemp fiber reinforced hybrid composite. IOP Conf. Series: Materials Science and Engineering 149 (2016) 012093 doi:10.1088/1757-899X/149/1/012093.

3   C. C. Chiao Aramid Fibers and Composites Handbook of Composites pp 272-317 Cite as Springer link

4   Z. Denchev Manufacturing and Properties of Aramid Reinforced Polymer Composites In book: Synthetic Polymer-Polymer Composites, Edition: 2012.

5   Narayan Prasad Sahu Study On Aramid Fibre and Comparison With Other Composite Materials IJIRST –International Journal for Innovative Research in Science & Technology| Volume 1 | Issue 7 | December 2014.

6   Gonzalo Pincheira influence of aramid fibre on the mechanical behavior of a hybrid carbon aramid reinforced epoxy composite https://doi.org/10.1177/1464420715612827

7   M Łach Mechanical properties of geopolymers reinforced with carbon and aramid long fibers IOP Conf. Series: Materials Science and Engineering 706 (2019) 012011 doi:10.1088/1757-899X/706/1/012011.

8   Irena Živković Analysis of Smart Aramid Fiber Reinforced Laminar Thermoplastic Composite Material Under Static Loading Scientific Technical Review,Vol.LVIII,No.1,2008

9   Muthukannan Rajkumar Design, Fabrication and Analysis of Advanced Polymer Based Kevlar-49 Composite Material. Applied Mechanics and Materials Vols. 592-594 (2014) pp 122-127 Online available since 2014/Jul/15 at www.scientific.net © (2014) Trans Tech Publications, Switzerland doi:10.4028/www.scientific.net/AMM.592-594.122.

10   P.N.B. Reis, J.A.M. Ferreira, P. Santos, M.O.W. Richardson, J.B. Santos, Impact response of Kevlar composites with filled epoxy matrix. Composite Structures 94 (2012) 3520–3528

Comparative Study of Mechanical Properties of Hybrid Composites using Carbon Fiber with Jute and Hemp

K.V. Manjunath

Department of Mechanical Engineering

K.S. Institute of Technology,

Bengaluru

Krishnamurthy. N

Department of Mechanical Engineering

Vijaya Vitala Institute of Technology,

Bengaluru

Abstract:- **Materials play vital role for the development of human being living standards. Hybrid composites are multi-phase system consisting of matrix and reinforcing material. This paper deals with the comparative study of hybrid composite material made up of carbon fibre with jute and carbon fibre with hemp which are fabricated by hand layup technique using Lapox L12 epoxy and K6 hardener. The mechanical properties of the hybrid reinforced composites like tensile and flexural of the various specimens are determined using Universal Testing Machine as per ASTM standards. The results shows that hybrid composites prepared by hemp and carbon are having better tensile and flexural strength as compared with jute and carbon. The microstructure of the above said hybrid reinforced composite materials has been analyzed using SEM.**

Keywords : Carbon, Jute, Hemp, Hand layup, Epoxy, Lapox L12, SEM.

1. INTRODUCTION

Composites can be defined as materials that consist of two or more physically and chemically different phases separated by a distinct interface at the macro level. Composites have the advantages such as low weight, corrosion resistance, high fatigue strength and faster assembly. They are extensively used in aircraft industries, packaging of medical equipment, space vehicle and sports goods. Hybrid composites are the combination of materials differing in composition, fibre type and these separate constituents act together to give the essential mechanical properties like strength and stiffness to the composite parts.

The matrix and reinforcement are the two main components that are essential in developing reinforced composites. These two phases consists of organic polymers as matrix and fibre as the reinforcement. Usually the strength and stiffness of the fibre are much higher than the matrix material, thus the fibre is the major load carrying component in polymer composites. The primary purpose of the matrix is to hold the fibre firmly and efficient load transfer which improves the mechanical properties of the reinforced composites. Natural fibre material mechanical properties make them an attractive ecological alternative to glass, carbon and manmade fibres used for the manufacturing of composites. These natural fibres are eco-friendly, available in nature abundantly and are renewable and economical. Due to these advantages the natural fibre composite materials have found many applications worldwide.

2. HYBRID COMPOSITE MATERIAL FABRICATION

There are many techniques available in industries for manufacturing of composite material such as hand layup technique, compression technique, vacuum bagging, resin transfer molding etc., The hand lay-up process of manufacturing is one of the most simplest and easiest methods for manufacturing composites. The primary advantage of the hand layup technique is to fabricate very large and complex parts with reduced manufacturing time. It is shown in Fig. 1.
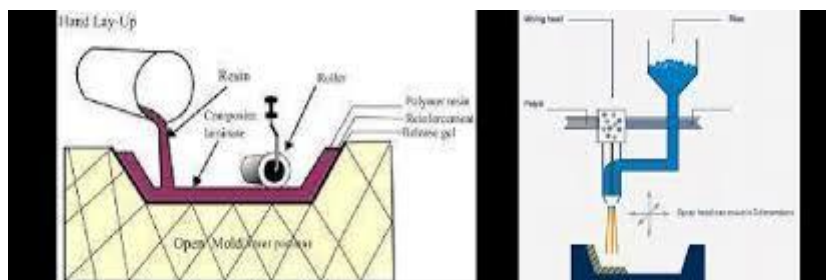

Fig. 1 Shows the hand layup technique for the fabrication of composite material

2.1 Experimental work

All experimental tests are carried out at Composite Technology Park Bangalore. All experimental tests were repeated to generate the data.

2.2. Tensile Test

Tensile test is one of the fundamental tests in material science in which the sample is subjected to a controlled tensile failure. The results are used to predict how the material will react under tensile loading. Some of the mechanical properties that are directly measured by tensile test are tensile strength, Young's modulus, and yield strength. This test is commonly used for obtaining mechanical properties of isotropic materials. Fig.2 shows the UTM with tensile specimen.
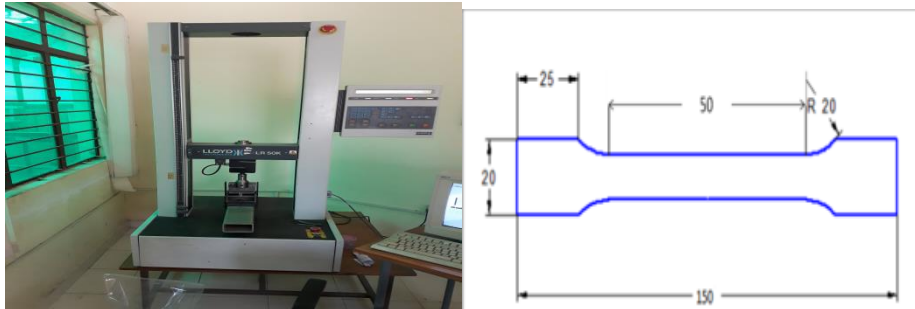

Fig. 2. Shows the UTM with tensile specimen

2.3 Flexural test

The three-point bending flexural test provides values for the modulus of elasticity in bending, flexural stress, flexural strain and the flexural stress–strain response of the material. The main advantage of the three-point flexural test is the ease of the specimen preparation and testing. However, this method has also some disadvantages. The results of the testing method are sensitive to specimen, loading geometry and strain rate. Fig.3. shows the UTM with flexural specimen.
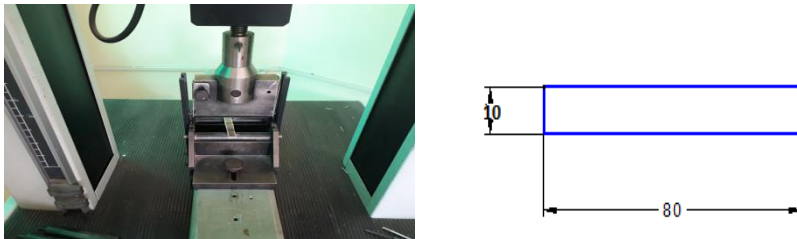

Fig.3. Shows the UTM with flexural specimen

2.4 SEM analysis

A scanning electron microscope is a type of electron microscope that produces images of a sample by scanning the surface with a focused beam of electrons. The electrons interact with atoms in the sample thus producing various signals that contain information about the surface topography and composition of the sample. SEM can achieve resolution better than 1 nanometre. SEM samples are prepared to withstand the vacuum conditions and the high energy beam of electrons and have to be small enough to fit on the specimen stage. Samples are generally mounted rigidly to the specimen holder using a conductive adhesive. Fig.4 shows the SEM analysis equipment.

Fig.4. Shows the SEM analysis equipment

3. RESULTS AND DISCUSSIONS

Experiments were conducted to determine the tensile strength, fleural strength and hardness of the above said material. All experimental tests were repeated three times to generate the data. The SEM analysis has been carried out to understand the internal structure of the hybrid composite material.

3.1 Tensile test results for Carbon and Jute Hybrid composite.

The mechanical behaviour of natural and synthetic fibres was investigated. Fig. 5 shows the tensile strength and Young's modulus of the hybrid composites prepared using carbon and jute. It was found that the average tensile strength to be 90.63MPa and the corresponding average Young's modulus to be 6422 MPa.
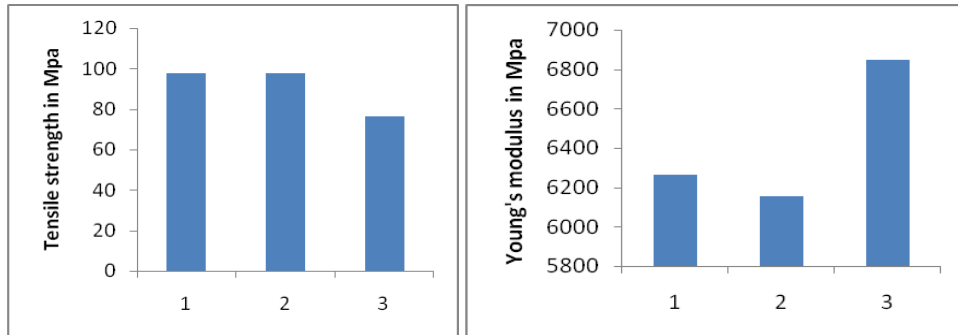

Fig.5 Shows the tensile strength and Young's Modulus of the composite material

3.2 Flexural test results for Carbon and Jute Hybrid composite.

Fig. 6 shows the flexural strength and its corresponding Young's modulus of the hybrid composite prepared by carbon and jute. It was found that the average flexural strength to be 322.93MPa and the corresponding average Young's modulus to be 1850.33MPa.
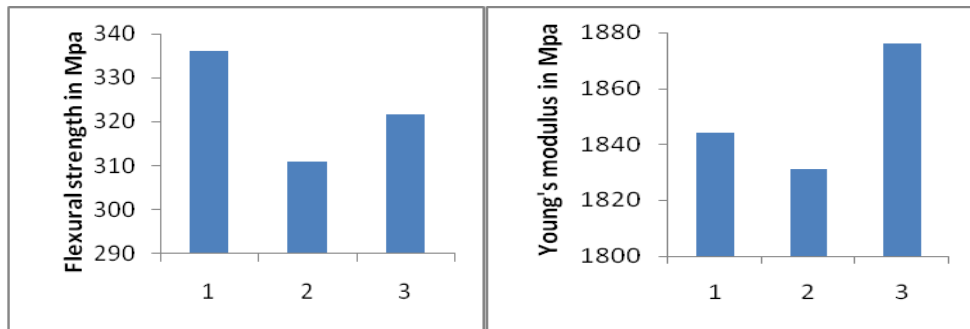

Fig.6 Shows the Flexural strength and Young's Modulus of the composite material

3.3 Tensile test results for Carbon and Hemp Hybrid composite.

The mechanical behaviour of natural and synthetic fibres was investigated. Fig. 7 shows the tensile strength and Young's modulus of the hybrid composite prepared using carbon and hemp. It was found that the average tensile strength to be 103 MPa and the corresponding average Young's modulus to be 8916MPa.

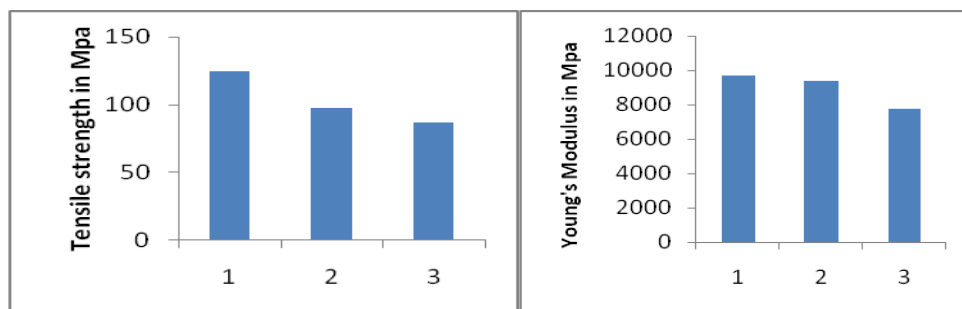Fig.7 Shows the tensile strength and Young's Modulus of the composite material

3.4 Flexural test results for Carbon and Hemp Hybrid composite.

Fig.8 shows the flexural strength and its corresponding Young's modulus of the hybrid composites prepared by carbon and hemp. It was found that the average flexural strength to be 335.33 MPa and the corresponding average Young's modulus to be 2653.66MPa.
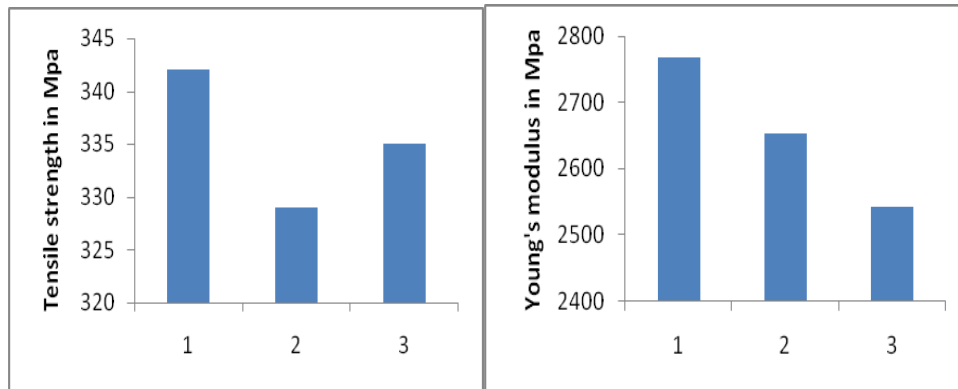
Fig.8 Shows the tensile strength and Young's Modulus of the composite mateial

3.5 SEM Analysis of hybrid composite materials

The microstructure of the fractured surfaces of carbon and jute, carbon and hemp are presented in Fig 9 with a magnification of 100X. It is evident from the microstructure that there is a fibre pull out, indicating the poor bonding between fibres and epoxy. This poor interfacial bonding reduces the mechanical properties of the composite materials.

Fig. 9 Shows tensile fracture of hybrid composites using carbon-jute and carbon-hemp

CONCLUSIONS

➤ Fabrication of multi layered reinforced hybrid composites using Carbon-Jute, Carbon-Hemp with epoxy has been successfully carried out using hand layup technique.

➤ It was observed that mechanical properties of the hybrid composites depend on the type of fibre and orientation.

➤ It was observed that carbon with hemp has yielded better results as compared to carbon and jute since hemp has better tensile strength than jute.

➤ Micro structure of the above said composite is observed using SEM. The fractured surface has shown the presence of voids and debris in case of hand layup technique.

REFERENCES

[1]   M R Sanjay "Studies on Mechanical Properties of Jute/E-Glass Fiber Reinforced Epoxy Hybrid Composites Journal of Minerals and Materials Characterization and Engineering", Vol. 4, Pages 15-25 published Online January 2016 in Scientific Research.

[2]   M. Muthuvel , G. Ranganath , K. Janarthanan K. Srinivasan "Characterization Study Of Jute And Glass Fiber Reinforced Hybrid Composite Material International Journal of Engineering Research & Technology" (IJERT), Vol. 2, Issue 4, April – 2013.

[3]   Navjot Pal Singh, Lakshay Aggarwal, V.K.Gupta (2015) study on 'Tensile Behaviour of Sisal/Hemp Reinforced High Density Polyethylene Hybrid Composite' Materials Today: Proceedings 2 (2015) 3140 – 3148

[4]   R. Bhoopathi, M. Ramesh,*, C. Deepa (2014) study on 'Fabrication and Property Evaluation of Banana-HempGlass Fiber Reinforced Composites' Procedia Engineering 9(2014)2032–2041

[5]   Asim Shahzad Hindawi Publishing Corporation Advances in Materials Science and Engineering Volume 2013, Article ID 325085, 9 pages

[6]   Subhash Kumar Gupta (2014) study on mechanical behavior of bamboo fiber based polymer composites Thesis, NIT Rourkela

[7]   Avtar Singh Saroya and Vishvendra Meena (2011) Study on 'study of mechanical properties of hybrid natural fiber composite' thesis, National Institute of Technology Rourkela.

[8]   Supriya Kunwar, Dr. K. K. S. Mer, Amit Joshi (2015) study on 'Mechanical Characterization of Graphene based Hybrid Polymer' international Journal of Scientific & Engineering Research, Volume 6.

[9]   V. Manikandan, P. Amuthakkannan, V. Arumuga Prabu (2015) study on 'Banana/Hemp Fiber and Its Hybrid Composites' Report number: Vol. 1: Issue 2, Affiliation: International Journal of Composite Material and Matrices

[10]   Gangadhar M Kanaginahal, Anjan Kumar Muniraju, Mr. Madhav Murthy (2014) study on 'Testing of Polymer matrix Hybrid Composites' Materials Today: Proceedings 00 (2014)

Performance Improvement on Biopolymer Nanocomposites

A.Hareesh
Associate Professor,
Amruta college of Engg and Management Science,
Bidadi, Bangalore-62109

Dr. M S Muruli
Principal,
ACS College of Engineering,
Bangalore

Dr. A Ramesha,
Principal,
BIT Institute of Technology,
Hindupur, Anantpur District

Ranganath N
Assistant Professor,
K S Institute of Technology,
Bangalore

Dr. Panchakshari H V
Professor,
Sri Venkateshwara College of Engineering,
Bangalore

Abstract— In this study, we investigated the effect of nano filler material on the mechanical and thermal property of biopolymer. For the preparation of specimens, solvent casting technique was used. Specimens are prepared using pure polylactic acid (PLA) with chloroform and Polylactic acid combined with nanoparticles (Clay). Moisture absorption results show that PLA Nanocomposite plays a great role in increasing the composite properties such as mechanical properties, since as the proportion of PLA Nanocomposite increase water uptake by the nano composite was less. nano composites produced by this method shows very good biodegradation behavior, which renders them advantageous in terms of environmental protection. OTR and WVTR test values show that PLA Nanocomposite plays a powerful role in increasing the gas barrier properties. Hence these PLA nanocomposites can be used for packaging to protect food from oxidation reaction and moisture.

Keywords-component; biopolymer, Polylactic Acid, nanoclay, chloroform, nanocomposite, Mechanical & Thermal Properties

I. INTRODUCTION

Poly lactic acid (PLA) has gained a considerable interest due to its biodegradability and biocompatibility. Poly lactic acid (PLA) is rigid thermoplastic polyester with a semi crystalline or completely amorphous structure depending on the stereo purity of the polymer backbone. Furthermore, its ability to be crystallized under stress, thermally crystallized, filled, and copolymerized, makes it suitable for a wide range of applications. The principal drawbacks of such a biodegradable polymer in terms of industrial application like food packaging are its poor thermal resistance, low mechanical and limited gas barrier properties. These properties can be improved by fillers, copolymerization techniques and by blending. However, the use of fillers appears to be the most attractive approach because of lower cost ease of Use.

Various candidate fillers for PLA are fiber-like natural fillers and other agricultural waste into polymeric matrix. Earlier studies have shown that presence of the natural fillers in biodegradable polymers may strongly accelerate biodegradation process. Moreover, presence of natural filler increases water absorption, which highly influences biodegradation process of the composites, in comparison to neat polymer. During the last decade, an increasing attention has been paid to biodegradable polymers because of environmental impact. Poly lactic acid (PLA) is a well-known green polymer produced from renewable resources that draws a lot of attention in the polymer industry. Several poly lactide properties such as mechanical strength, thermal stability and permeability need to be improved in order to enlarge its range of applications, especially in packaging, since PLA is too much brittle and permeable to gases for some purposes. The introduction of a few percent of nano fillers, such as layered alumino silicate clays, is known to enhance various polymer properties such as the stiffness/toughness balance.

Nano particle fillers

It has been reported that addition of nanoparticles to base polymers confers improved properties that make them usable in automotive, construction and medical areas. PLA nanocomposites have been shown to exhibit improved tensile strength and young's modulus compared to Pure PLA. Nanocomposites are a class of composites in which the dimensions of the reinforcing material are in the order of nanometers. Compared to conventional composites nano filler composites exhibit superior properties due to better interfacial bonding. Several nano filler materials such as calcium carbonate, ceramic, clay, graphite, kaolin, mica etc., have been tried out to obtain nano composite materials. Nano clay is a good candidate for use as a filler material due to its remarkable increase in rigidity (elastic modulus), thermal and dimension stability, good barrier properties to gases and vapours, toughness. Depending on the specific interactions between the polymeric matrix and the clay, different structures such as intercalated and exfoliated may be obtained. The clay layers may be well dispersed provided that a strong interaction can be developed between the clay and the polymeric matrix.

II. MATERIALS AND METHODS

PLA with a density of 1300 kg/m^3, melting point of 150-170 °C and molecular weight (M_w) of 197000 g/mol. PLA resins were dried in a vacuum oven at 60 °C for 24 hours before use. Organically modified fillers as Nano reinforcement, Solvents was used to dissolve PLA and to swell and disperse Nano reinforcement, Glycerol was used to grease the molds prior to casting

Special Issue - 2019

International Journal of Engineering Research & Technology (IJERT)
ISSN: 2278-0181
NCRAEM - 2019 Conference Proceedings

Method of preparation:

- In the first step of preparing the specimen, 10gms of PLA were dissolved in 100ml of chloroform solution and it is poured into a glass beaker.
- In the second step, the solution was stirred vigorously on a magnetic stirrer for dissolving the PLA into the solution for 5hrs. At the same time nano clay of 1gm was added into the solution mixture.
- In the third step, Dissolved solution was poured onto a greased glass molds and allowed to dry for 24hrs at room temperature

Preparation of films

PLA and PLA-based nanocomposites films were prepared using a solvent casting method as shown in fig 1. 10gms of PLA was dissolved in 100 mL of solvents while agitating vigorously for 5 hours at room temperature (25°C). The dissolved solution was poured onto greased glass molds and then allowed to dry for about 24 hours at room temperature. The manufactured film was removed from the casting surface. For the preparation of PLA nanocomposite films, a predetermined amount of fillers was dispersed in the solvent by vigorous stirring for 5 hours with a magnetic stirrer. They were then homogenized at 2,000 rpm for 45 min followed by sonication for 30 min at room temperature. The filler solutions were mixed with the previously prepared PLA solution and then stirred for 15 min with a magnetic stirrer. The solutions were homogenized at 2,000 rpm for 45 min and sonicated for another 30 minutes, then casted onto greased glass molds. The final film was obtained by the same procedure explained above for pure PLA films. After drying at room temperature for 24 hours, all PLA films were further dried at 60°C in a vacuum dryer to remove the remaining solvent to prevent its plasticizing effect.

Fig 1: PLA Film Preparation of size 200mmx150mm

Material Properties

Moisture absorption behavior

The moisture absorption results are crucial for understanding the performance of cellulose-based composites, since the moisture pickup under immersion in water or exposure to high humidity, intimately relates to such composite properties as mechanical strength, dimensional stability and appearance. Though the poly(lactic acid) has been considered as one of the most promising materials for biodegradable plastics, but because of its poor resistance to water absorption limits its wide applications. Addition of fillers is an effective way of decreasing its sensitivity to moisture and improving mechanical properties. Moisture absorption test was carried for all the ten composite films in which the PLA Nanocomposite and matrix polylactic acid are in the ratio of 10:90, 20:80, 30:70, 40:60, 50:50, 60:40, 70:30, 80:20, 90:10 and 95:05. It was observed that as the percentage of PLA Nanocomposite increases, moisture absorption decreased. This behavior clearly reflects the presence of hydrophobic moieties onto the fibre surface increase in their resistance towards moisture.

Biodegradation in soil

Biodegradation of materials occurs in various steps. Initially, the digestible macromolecules, which join to form a chain, experience a direct enzymatic scission. This is followed by metabolism of the split portions, leading to a progressive enzymatic dissimilation of the macromolecule from the chain ends. Oxidative cleavage of the macromolecules may occur instead, leading to metabolization of the fragments. Either way, eventually the chain fragments become short enough to be converted by microorganisms.

The studies on biodegradation behavior are important for the application of biocomposites in environment. In this work, soil burial experiments were performed for all the ten ratio films. Table 1 shows present weight loss of various films as a function of biodegradation time. Note that weight loss shows an approximately linear relation with degradation time for all the ten films. For all the films, weight decreases for 2 days is average 3% and it decreases gradually as the time increase and after 18 days average weight decrease is 16%. The ability of films to degrade depends greatly with physico-chemical characteristics of the substrate, such as the degree of crystallinity and polymerization of cellulose, of which the crystallinity degree of cellulose is the most important structural parameters. Crystalline regions are more difficult to degrade. All the ten film composites showed almost same resistance to microorganism attack in the soil. As the microorganism attacks, the composites lose their structural integrity. Undoubtedly, the results obtained to herein reveal that the film composites would not cause any deleterious ecological impact.

Table1: Moisture absorption studies of ten (PLA Nanocomposite/PLA) film composites

No. of days	%wt. increase 10:90	%wt. increase 20:80	%wt. increase 30:70	%wt. increase 40:60	%wt. increase 50:50	%wt. Increase 60:40	%wt. increase 70:30	%wt. increase 80:20	%wt. increase 90:10	%wt. increase 95:05
2	2.9	2.7	2.7	2.4	1.9	1.7	1.7	1.5	1.4	1.4
4	5.1	4.9	4.8	4.4	3.9	3.6	3.6	3.1	2.9	2.8
6	7.2	6.9	6.7	6.2	5.6	5.1	5.0	4.5	4.3	4.2
8	9.0	8.7	8.4	7.8	7.1	6.5	6.4	5.9	5.6	5.5
10	10.6	10.3	9.7	9.0	8.2	7.5	7.3	6.8	6.4	6.2
12	12.3	12.0	11.0	10.1	9.3	8.6	8.2	7.7	7.2	6.9
14	13.9	13.5	12.2	11.3	10.4	9.6	9.1	8.6	8.0	7.6
14	13.9	13.5	12.2	11.3	10.4	9.6	9.1	8.6	8.0	7.6
16	15.7	15.3	14.5	12.5	11.4	10.7	10.1	9.4	8.7	8.2
18	17.2	16.7	15.8	13.6	12.5	11.8	11.0	10.2	9.5	8.9
20	18.6	18.1	17.1	14.8	13.6	12.9	11.9	11.1	10.2	9.5
22	20.1	19.5	18.3	16.0	14.7	13.9	12.8	12.0	11.0	10.1
24	21	20.3	19.5	17.2	15.7	14.9	13.8	12.8	11.7	10.6

Table 2: Biodegradable studies of ten (PLA Nanocomposite/PLA) film composites

No. of days	%wt. decrease 10:90	%wt. decrease 20:80	%wt. decrease 30:70	%wt. decrease 40:60	%wt. decrease 50:50	%wt. decrease 60:40	%wt. decrease 70:30	%wt. decrease 80:20	%wt. decrease 90:10	%wt. decrease 95:05
2	2.7	2.8	3.0	2.9	2.8	3.1	2.9	3.0	3.3	3.2
4	3.9	3.8	4.1	3.9	3.9	4.2	3.7	4.2	4.2	4.4
6	5.8	5.6	5.9	5.7	5.5	5.6	5.3	5.5	5.7	5.6
8	7.7	7.5	7.6	7.4	7.5	7.4	7.7	7.6	7.8	7.6
10	9.3	9.5	9.4	9.2	9.3	9.6	9.6	9.8	9.7	9.8
12	11.7	11.6	11.7	11.5	11.4	11.6	11.4	11.6	11.7	11.9
14	13.2	13.4	13.6	13.7	13.5	13.8	13.7	13.8	13.9	14.0
16	15.4	15.7	15.6	15.9	15.4	15.6	15.6	15.7	15.5	15.7
18	15.6	15.8	15.7	15.9	15.5	15.6	15.8	15.8	15.6	15.9

Oxygen permeability test

Oxygen permeability depends on chain flexibility, phase and physical state of the polymer and packing of its molecules. The most permeable polymers are amorphous, with very flexible chains, in a high elastic state. The gas permeability of crystalline polymer is much lower. The high molecular weight glassy polymers with rigid chains have very low gas permeability. With decreasing chain flexibility gas Permeability decreases. Closer packing of the molecules supports permeability resistance.

Table 3 shows represent OTR (Oxygen Transmission Rate) values for all the ten ratio films. Generally, hydrophilic polymeric films have shown good oxygen barrier property. As it can be observed in Figure 4.15, there was an improvement in oxygen barrier properties of the films as the percentage of PLA Nanocomposite increases. It was observed that there is a great decrease in oxygen transmission rate as the percentage composition of the PLA Nanocomposite increases. It is obvious that PLA Nanocomposite played a powerful role in improving the oxygen gas barrier properties. The increased molecular interaction resulted in a film with compact structure and low OTR value. Oxygen Transmission Rate increases as

the percentage of PLA Nanocomposite decreases because intermolecular bonding between fibre and matrix decreases. This resulted in a phase separation among the main components where the film could not be formed well, facilitating the oxygen permeation. So, it was more advantageous to improving the gas barrier properties by increasing the percentage of PLA Nanocomposite. This result indicates the potential of these films to be used as a natural packaging to protect food from oxidation reactions.

Table 3: OTR values of ten (PLA Nanocomposite/PLA) film composites

SL No	PLA Nanocomposite+ Pure PLA	OTR value; Cc/sqm/day/atm
1	10+90	1850
2	20+80	1698
3	30+70	1520
4	40+60	1423
5	50+50	1315
6	60+40	1220
7	70+30	1105
8	80+20	1090
9	90+10	980
10	95+5	823

composition of PLA Nanocomposite increases, hydrophilicity of the film decreases. This phenomenon could be related to the significant hydrogen bonding interaction with water. The comparison between OTR and WVTR indicates that PLA Nanocomposite is greatly effective in obstructing the oxygen permeation, but less effective in retarding the water vapour permeation. This results shows that these films may impede moisture transfer between the surrounding atmosphere and food, or between two components of a heterogeneous food product. This property is very much use full in packaging application.

Table 4: WVTR values of ten (PLA Nanocomposites/Pure PLA) film composites

SL NO	PLA Nanocomposite+PLA	WVTR value gm/sqm/day
1	10+90	6.532
2	20+80	5.842
3	30+70	5.023
4	40+60	4.492
5	50+50	4.12
6	60+40	3.658
7	70+30	2.98
8	80+20	2.845
9	90+10	2.059
10	95+5	1.234

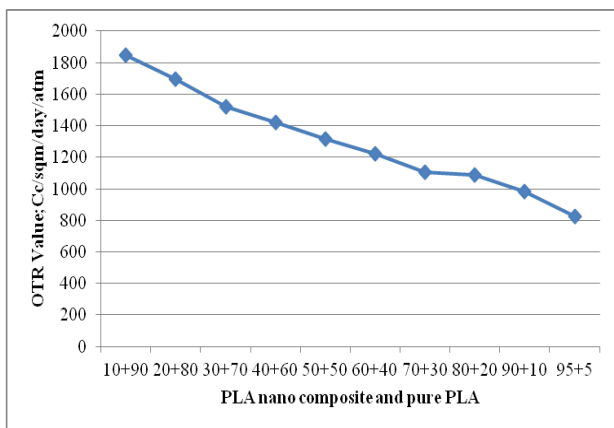

Figure 2: Oxygen permeation versus Parts per hundred PLA nanocomposites in a (PLA Nanocomposite/Pure PLA) blend
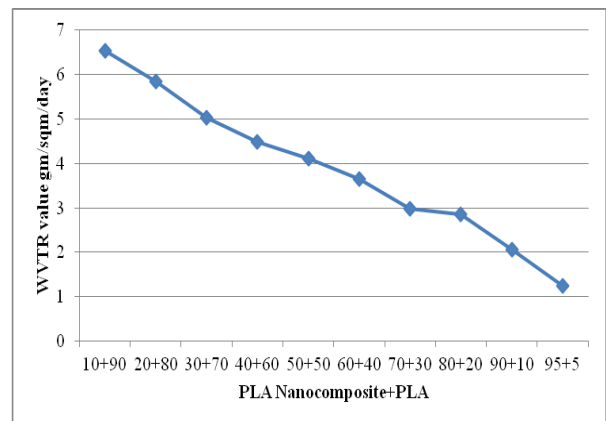

Figure 3: Water vapour permeation versus Parts per hundred PLA Nanocomposite in a (PLA Nanocomposite/PLA) blend

Water vapour permeability test
Table represents Water Vapour Transmission Rate values for all the ten ratio films. The water vapor permeability of films depends on many factors, such as the integrity of the film, the hydrophilic-hydrophobic ratio, the ratio between crystalline and amorphous zones and the polymeric chain mobility. It was observed that there is a small decrease in water vapour transmission rate as the percentage composition of the PLA Nanocomposite increases. This is because as the percentage

conclusion

- Moisture absorption results show that PLA Nanocomposite plays a great role in increasing the composite properties such as mechanical properties, since as the proportion of PLA Nanocomposite increase water uptake by the nano composite was less. nano composites produced by this method shows very good biodegradation behavior, which renders them

Special Issue - 2019

International Journal of Engineering Research & Technology (IJERT)
ISSN: 2278-0181
NCRAEM - 2019 Conference Proceedings

advantageous in terms of environmental protection. The produced film composites possess higher tensile strength as the proportion of PLA Nanocomposite increases and higher elongation at break as the proportion of PLA increases. So PLA Nanocomposite plays a vital role in increasing the tensile strength of film composites.

- OTR and WVTR test values show that PLA Nanocomposite plays a powerful role in increasing the gas barrier properties. Hence these PLA nanocomposites can be used for packaging to protect food from oxidation reaction and moisture.

REFERENCE

[1] Heath Ledger, David Gilmore. "Polymer Testing." Polymer Science 27 (2008): 835-840.

[2] Lucky Sharma, G W Padua. "Nanocomposites in Food Packaging." Food Science 75 (2010): 43-49. https://doi.org/10.1111/j.1750-3841.2009.01456.x

[3] M.Yang, B.Li. "Polymer Composites." Polymer 17 (2006): 439-443.

[4] Roger Waters, A.V.Janorkar, D.E.Hirt. "Crystallization of PLA." Polymer Science 35 (2010): 338-356.

[5] Saeed Dadashi, Seyed Mohammad Ali Mousavi, Zahra Emam-Djomeh, Abdulrasoul Bob Oromiehie Marley. "Func. Prop. of Biodegradable Nanocomposites from PLA." Nanoscience Nanotechnology 10 (2014): 245-256.

[6] V Kumar, A.P.Guptha. "Synthetic Biodegradable Polymers." European
Polymer Journal 43 (2007): 4053-4074.
https://doi.org/10.1016/j.eurpolymj.2007.06.045

[7] Rola Mansa, Chih-Te Huang, Ana Quintela, Fernando Rocha, Christian
Detellier. (2015), "Preparation and characterization of novel clay/PLA
nanocomposites", Applied Clay Science, 115, 87–96
https://doi.org/10.1016/j.clay.2015.07.024

[8] Najafi, N., Heuzey, M.C., Carreau, P.J, (2012), "Polylactide (Pla)-Clay Nanocomposites Prepared By Melt Compounding In The Presence Of A Chain Extender", Composites Science and Technology,   72,   608-615
https://doi.org/10.1016/j.compscitech.2012.01.005

[9] Teuku Rihayat, Suryani Salim, Harry Agusnar, Fajri and Zaimahwati
(2015), "Synthesis of polyurethane/clay nanocomposites based palm oil polyol coating", Journal of Mechanical Engineering and Sciences, 9, pp.
1580-1586 https://doi.org/10.15282/jmes.9.2015.5.0153

[10] Fiore V, Botta L, Scaffaro R, Valenza A, Pirrotta A. PLA based biocomposites reinforced with Arundo donax fillers. Compos Sci Technol 2014;105:110-7

[11] Scaffaro R, Lopresti F, Botta L, Rigogliuso S, Ghersi G. Preparation of threelayered porous PLA/PEG scaffold: relationship between

[12] Byeong-UkNama,Kyung-DeokMina,YounggonSon
"Investigation of the nanostructure, thermal stability, and mechanical properties of polylactic acid/cellulose acetate butyrate/clay nanocomposites" MaterialsLetters150(2015)118– 121 , http://dx.doi.org/10.1016/j.matlet.2015.03.019

[13] Amita Bhatia, Rahul K. Gupta, Sati N. Bhattacharya, and Hyoung JinChoi "Analysis of Gas Permeability Characteristics ofPoly(LacticAcid)/Poly(ButyleneSuccinate)
Nanocomposites" Volume 2012, Article ID 249094, 11 pages, doi:10.1155/2012/249094

[14] Wenhui Li, Lin Li , Yun Cao, Tianqing Lan "Effects of PLA Film Incorporated with ZnO Nanoparticle on the Quality Attributes of Fresh-Cut Apple" Nanomaterials **2017**, 7, 207; doi:10.3390/nano7080207

[15] nanoclayAyana B., Supratim Suin, B.B. Khatua "Highly exfoliated eco-friendly thermoplastic starch (TPS)/poly (lacticacid)(PLA)/clay

nanocomposites using unmodified nanoclay" Carbohydrate Polymers   110   (2014)   430–439   , http://dx.doi.org/10.1016/j.carbpol.2014.04.024

[16] Byeong-Uk Nam, Kyung-Deok Min, YounggonSon "Investigation of the nanostructure, thermal stability, and mechanical properties of polylactic acid/cellulose acetate butyrate/clay nanocomposites" MaterialsLetters150(2015)118– 121, http://dx.doi.org/10.1016/j.matlet.2015.03.019

[17] K. Fukushima, A. Fina, F. Geobaldo, A. Venturello, G. Camino "Properties of poly(lactic acid) nanocomposites based on montmorillonite, sepiolite and zirconium phosphonate" Vol.6, No.11 (2012) 914–926, DOI: 10.3144/expresspolymlett.2012.97

Investigation of microstructural, tensile and hardness characteristics of Aluminium 2024 alloy based Metal Matrix Composites

[1]N.Sreesudha, [2]N. Krishnamurthy, [3]M.S. Murali

[1]*Asst. Professor Department of Mechanical Engineering*
K.S.Instituteof Technology, Bengaluru, Karnataka, India
[2]*Professor & Head, Department of Mechanical Engineering,*
Vijaya Vittala Institute of Technology, Bengaluru, Karnataka, India
[3] *Principal, ACS College of Engineering*
Bengaluru, Karnataka,India

Abstract - In this present investigation, efforts are made to study the micro structure, tensile strength and hardness of Al2024 composites with SiC / TiC particulates reinforced. The vortex method of stir casting was employed, in which the reinforcements were introduced into the vortex created by the molten metal by means of mechanical stirrer. Castings were machined to the ASTM standards on a highly sophisticated lathe. The samples were subjected to microstructural study, tensile and hardness tests. The degree of improvement of tensile strength and hardness characteristics of MMCs is strongly dependent on the kind of reinforcement. An improved tensile strength and hardness characteristics occurs on reinforced compared to unreinforced MMCs alloys.

Key words: MMCs, Al 2024 matrix, Microstructure, Tensile strength, Hardness.

I. INTRODUCTION

In the present days much attention has been focused on Metal Matrix Composites (MMCs) mainly due to their superior properties. Aluminium based metal matrix composites (AMMCs) have good mechanical and physical properties and hence they are used in various applications [1]. AMMCs have low density, improved stiffness, high strength and improved high temperature properties [2]. Because of their superior properties, they are extensively applied in the field of aircraft, spacecrafts, automobiles with the parts such as engine piston, electronic packaging, brake drums and so on [3]The wear resistance, hardness abrasive property, strength to weight ratio and thermal properties of AMMCs can be further improved by the reinforcement of hard particles like ceramics.The unique properties of the particulate reinforced composite materials are to a great extent dependent on the unique nature on the matrix-particle interface. The most common material reinforcements are Al2O3and SiC [4].The improvement in the mechanical properties are influenced by the type of the particle, morphology, size, volume fraction and distribution of the reinforcing particles in the base metal matrix[5]. When hard ceramic particles are added to soft Aluminium alloys, it enhances the wear strength and wear resistance [6].Reinforcement disbursement should be uniform throughout the composite material in order to achieve high strength which, otherwise leads to lower strength, lower ductility and toughness due to clusters of reinforcement [7].The grain size and the percentage of reinforcement influences in selection of the fabrication method of the composite.

AMMCs are produced using stir casting method , Friction stir processing and powder metallurgy techniques[8].Out of all the processes, stir casting process is the most economical and effective method to produce particulate reinforced metal matrix composites. Mechanical stirring in the furnace is the key element in stir casting process to get the dispersion of ceramic particles and sufficient wetting of the particles by the liquid metal [9].The distribution of ceramic particles depends upon the geometry of stirrer, speed of the stirrer placement of stirrer in the furnace and melt temperature in furnace[10]

After extensive literature survey, it is observed that the improvement in tensile strength and wear properties of Aluminium based metal matrix composites are resulted with the addition of different weight percentages of reinforcements, their grain size, shape, different fabrication methods [11-14]. From previous investigations it is observed that SiC with Flyash reinforced Aluminium hybrid composites exhibits better mechanical properties with lower density and porosity level compared to unreinforced Aluminium composites [15-17].

Cao Fenghong et. Al Studied that the hardness of hybrid composite of Al 6061/SiC/WC composite has been increased due to the incorporation of stiffer and stronger reinforcement in the matrix material [18].It is generally

observed the addition of ceramic particles in different proportions improves different mechanical thermal and tribological properties of base Aluminium matrix[19-20].

The main objective of this project is to develop Al (2024)-Silicon carbide/Titanium carbide particulate metal matrix composites. The silicon carbide/ Titanium Carbide is used as the reinforcement & Al 2024 is used as matrix material. Different weight percentage of composite specimens areprepared by using liquid route metallurgy technique. Test specimens are prepared and are evaluated for their tensile and hardness characteristics.

II. EXPERIMENTATION

2.1 Selection of material

The matrix material Al 2024, reinforcement material SiC30-40 μm size particles /TiC 30-40 μm are used for the development of MMCs. The chemical composition of Al2024 is as shown in the Table 1.

Table 1: Al 2024 Chemical composition

Element	Copper	Magnesium	Manganese	Iron	Silicon	Chromium	Zinc	Aluminum
Weight percentage (Wt%)	4.3	1.3	0.4	0.4	0.3	0.1	0.3	93

2.2 Preparation of Composite

The SiC/TiC of 30-40 μm size were used as the reinforcement and the reinforcement content in the composites was varied from 0% to 8% in steps of 2% by weight. Liquid metallurgical technique was used to prepare the composite materials in which the SiC/TiC particles were added to the molten pool through a vortex created due to continuous stirring using an alumina coated stainless steel stirrer. Zirconium coated stirrer was also used to stir the molten metal. The pre-heated (7730K) SiC/TiC particles were added into the vortex of the liquid melt. The resulting mixture was poured by tilting the same in to the preheated permanent moulds. Figure 1 and 2 shows the stir casting process and casings respectively.

Figure:1 Stir casting equipment   Figure :2Castings

2.3. Study of microstructure

Examination of micro structure of prepared composites was done using scanning electron microscope to study and analyze the microstructure. A section of the castings was taken and were polished with different grades of emery papers. The samples were examined under scanning electron microscope.

2.4. Tensile test

Tensile tests were carried out at room temperature as per ASTM E8. The geometry of tensile test specimen is shown in Fig. 2.3. The prepared tensile test specimens are shown in Fig. 2.4. The test uses specimens of 20 mm grip diameter, 30 mm grip length, 62.5 mm gauge length, 75 mm length of reduced cross section, inner diameter of 12.5 mm fillet radius of 10mm and total length 155 mm were machined from those cast composites for the gauge length of the sample parallel of the longitudinal axis of the castings. The figure 3 shows the machined test specimens.
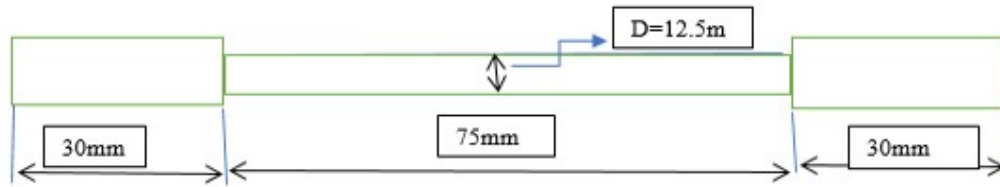
Figure: 3 Geometry of tensile test specimen

Figure: 4 Prepared Tensile specimens as per ASTM E8standard.

2.5. Hardness test

Brinell hardness test was performed by indenting a hard steel or carbide sphere of a specific diameter under a specific load into the surface of a material and measuring the diameter of the indentation left after the test. The Brinell Hardness Number (BHN) is calculated using the following formula. Figure 5 shows the specimens after Brinell hardness test.

$$BHN = \frac{F}{\frac{\pi}{2} D * (D - \sqrt{D^2 - Di^2})}$$

Where,

BHN = Brinell Hardness Number

F = Applied load in kg

D = Diameter of the spherical indenter in mm

Di = Diameter of the resulting indentation in mm

Fig.2.5 shows the hardness samples with indentation

Figure: 5Specimens after conducting Brinell's test

III RESULTS AND DISCUSSION

3.1 Microstructural Characterization

The SEM micrographs of Al 2024, Al2024+2 wt. % of SiC,Al2024 + 4 wt. % of SiC, Al2024 +6 wt. % of SiC and Al7075+8 wt. % of SiC are shown in Figure 6.In Al2024+2 wt. % of SiC sample, there is a uniform distribution of SiC ceramic particles in the Aluminum alloy base matrix in the form of grains. The grain formation patterns could be due to the orientation of reinforcements into the matrix caused by the stirring process, the density and other factors that influence the settlement of the reinforcement particles into the matrix material. In Al2024 + 4 wt. % of SiC sample the dispersion of the SiC particles are reasonably homogenous, while the formations of the grain patterns are comparatively finer. The micrograph of Al2024 +6 wt. % of SiC shows uniform distribution of the SiC particles in the Aluminium alloy matrix and refined grain structure is observed. In the micrograph of Al2024+8 wt. % of SiC.one can observe random grain orientation with clustering spots of ceramic particles which could be due to an increase in the weight percentage of silicon carbide/Titanium Carbide particles.The reinforcement particles are uniformly distributed by stirring process where dendrite shaped structure breaks into equiaxed form. This improves the wettability and incorporation of the particles within the melt. This method enables dispersion of reinforcement particles more uniformly in the matrix.

Figure 7 shows the SEM micrographs of Al 2024 with 2, 4, 6 and 8% by weight of Titanium carbide reinforcement. SEM micrographs shows the uniform distribution of Titanium carbide particles in the samples. The micrographs of 4 wt% and 6 wt% Titanium Carbide shows uniform distribution of the reinforced particles as well as agglomeration of particles at few places.
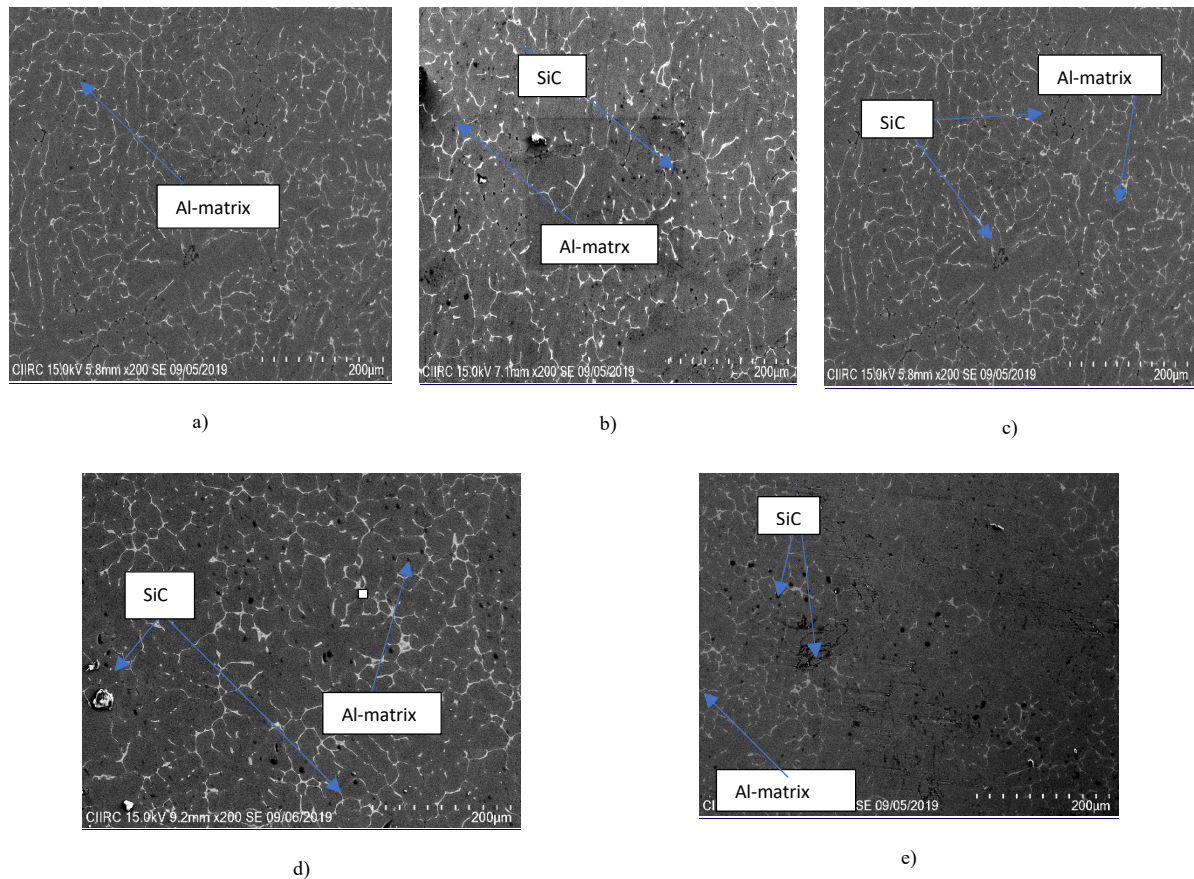

a)   b)   c)

d)   e)

Figure: 6SEM micrographs of Al 2024 alloy -SiC compositea) Al 2024+0% SiC AC , b) Al 2024+2% SiC AC, c) Al 2024+4% SiC AC, d) Al 2024+6% SiC AC, e) Al 2024+8% SiC AC
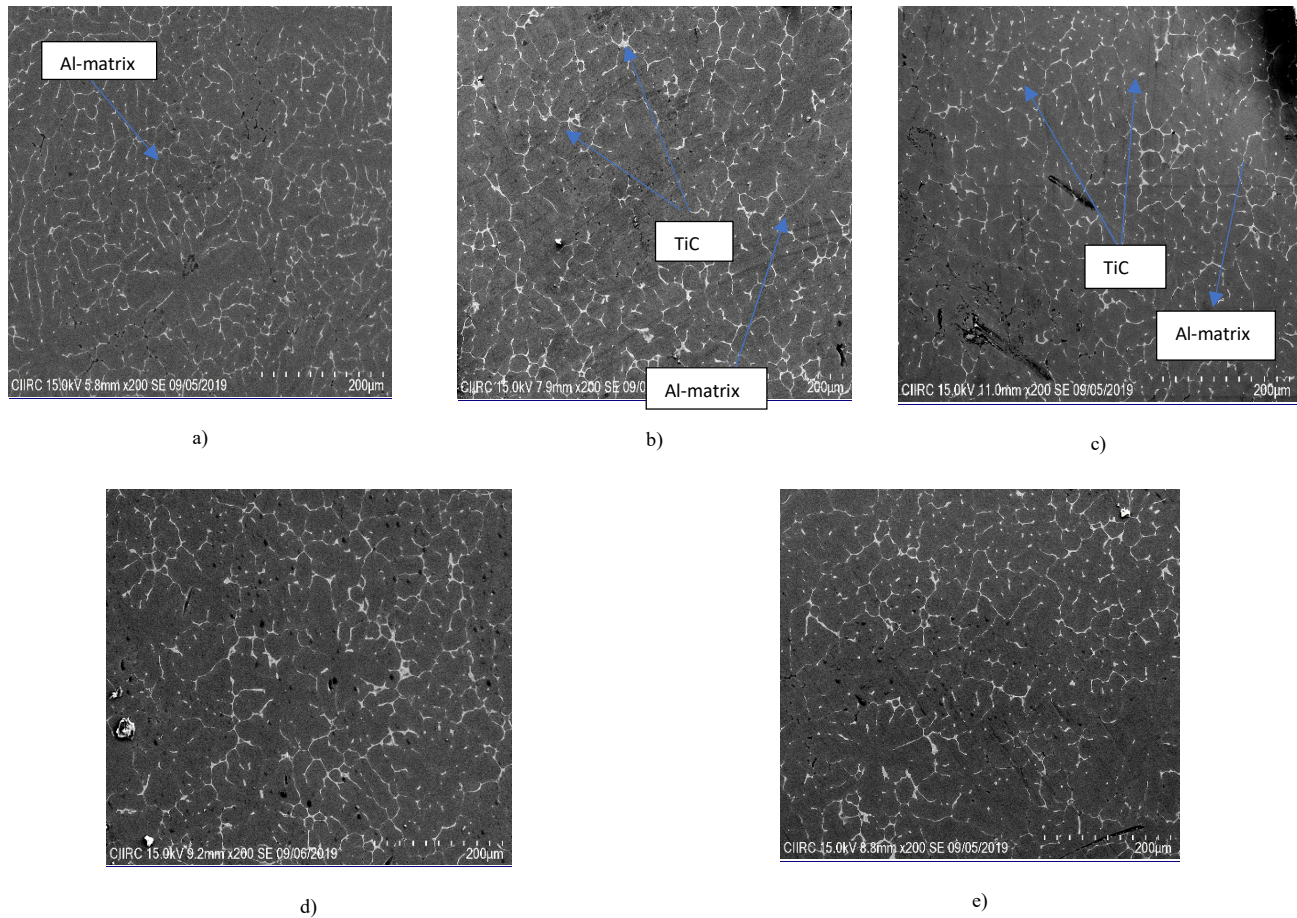
Figure 7 : SEM micrographs of Al 2024 alloy -TiC compositea) Al 2024+0% TiC ACb) Al 2024+2% TiC ACc) Al 2024+4% TiC AC

d) Al 2024+6% TiC ACe) Al 2024+8% TiC AC

3.2. Tensile properties

3.2.1 Effect of reinforcements on Ultimate Tensile Strength(UTS)

The variation of UTS with the percentage of reinforcement is shown in Figure 8.The reinforcing phase in the metal matrix composites has much higher stiffness than the matrix. The enhancement of elastic modulus and strength of the composites takes place due to the strong interface which transfers and distributes the load from the matrix to the reinforcement. The particle reinforced Al-MMCs possesses higher tensile strength than monolithic alloys. The tensile strength of the which is not reinforced is 185 N/mm^2 and this value increased to 210 N/mm^2 for Al/(6%SiC). In case of Al/TiC which makes the material stiffer than the Al-SiC particles, and the tensile strength increased to 217 N/mm^2.The main reason is Titanium Particles are distributed uniformly in composites and grain boundaries are very small, this in turn increases the strength of the composite.

Figure 8 : Reinforcement effect on UTS

3.2.2 Effect of reinforcements on percentage elongation

Figure 9 depicts the graph of the experimental elongation of the composites with different percentage of reinforcement. From the graph, it is observed that the elongation of composites gradually reduced as compared to unreinforced aluminium. For unreinforced Al elongation is seen as 16%.
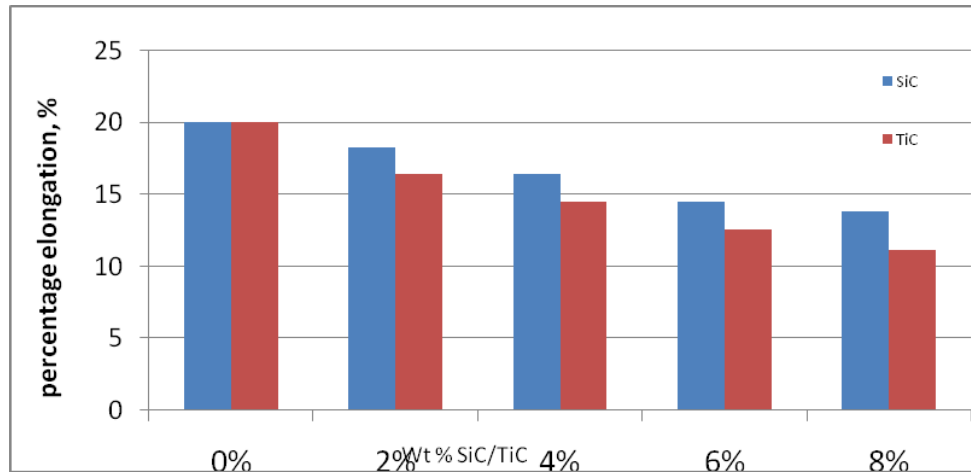

Figure 9: Reinforcement effect on percentage elongation

3.2.3 Influence of reinforcements on yield strength

Figure 10 shows the effect of reinforcement on yield strength. From the graph it is observed that an increase in the content of SiC particulates from 0% to 2% in the base matrix causes increase in yield strength by an average of 12%. Further an increase in SiC particulates from 2% to 4% yields an increase in yield strength about 14.28%. With 4% to 6% increase in reinforcement will increase yield strength by 9.89%. Further increase of reinforcement from 6% to 8% caused a decrease in yield strength by 55.23%. This is mainly due to cluster formation of SiC particulates in the base matrix.
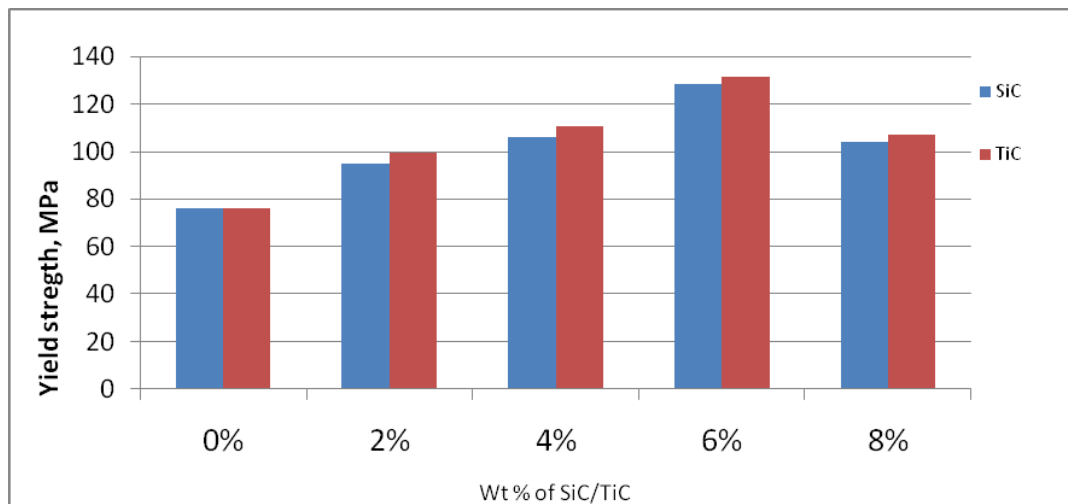

Figure 10: Reinforcement effect on yield strength

3.3 Hardness test results

Figure 11 shows the variation of BHN with percentage of reinforcement. It is noticed that an increase in the hardness with the increase in weight fraction of SiC/TiC. The maximum hardness is obtained for Al/(6%SiC/TiC)

sample. Thus, in conclusion, the mechanical properties such as yield strength, tensile strength and hardness of the composite increases with the increase in the reinforcement of SiC/TiC.
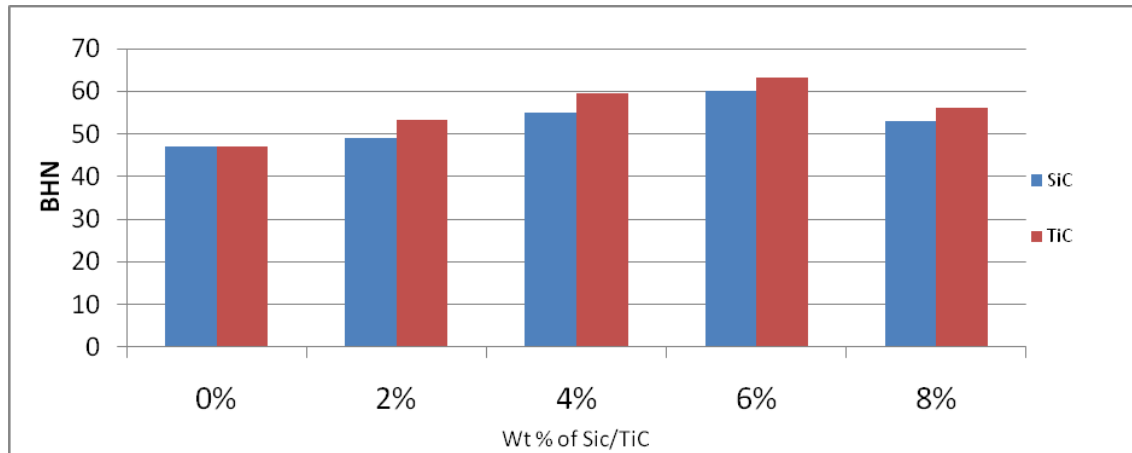

Figure 11:Reinforcement effect on hardness

IV CONCLUSIONS

1. Metal matrix composites with Aluminium 2024 as base matrix and reinforcement as SiC/TiC particles with various weight fraction were successfully synthesized by using stir casting method.

2. A remarkable improvement in micro hardness is noticed with increase in SiC/TiC particles in Al2024- SiC/TiC composite when compared with unreinforced alloy.

3. Though the ductility of the composites reduces with the addition of secondary particles in the aluminium alloy,however, Al2024 alloy have higher ductility when evaluated with the composites under all the compositions studied.

4. UTS of Al2024 alloy and Al2024- SiC/TiC composites increase with increase in reinforcement percentage.

REFERENCES

[1] AKM Asif Iqbal1, Dewan Muhammad Nuruzzaman,"Effect of the Reinforcement on the Mechanical Properties of Aluminium Matrix Composite: A Review" International Journal of Applied Engineering Research,2016,volume 11, issue 21, pp-10408-10413.

[2] M K Surappa, Sadhana, "Aluminium matrix composites: Challenges and opportunities" 2003, volume 28, pages 319–334.

[3] L Mahesh, M Vinyas, J Sudheer Reddy and B K Muralidhara,"Investigation of the microstructure and wear behaviour of titanium compounds reinforced aluminium metal matrix composites",2018,Materials Research Express, volume 6, Number 2.

[4] B. Vijaya Ramnath.et.al, "Aluminium metal matrix composites - a review'' Reviews on.Advance Material Science, 2014, volume 38,pp.55-60.

[5] C.Suryanarayana and Nasser Al-Aqeeli "Mechanically Alloyed Nanocomposites" Progress in Materials Science 2013, volume 58, pp.383–502.

[6] Md. Habibur Rahmana,*, H. M. Mamun Al Rashedb, "Characterization of silicon carbide reinforced aluminum matrix composites",Procedia Engineering 2014,volume 90,pp. 103 – 109.

[7] Pardeep Sharma, Gulshan Chauhan , Neeraj Sharma "Production of AMC by stir casting – An Overview", International Journal of Contemporary Practices ,volume.2, Issue1.pp.56-65

[8] Bagesh Bihari, Anil Kumar Singh "An Overview on Different Processing Parameters in Particulate Reinforced Metal Matrix Composite Fabricated by Stir Casting Process" Int. Journal of Engineering Research and Application, 2017, volume.7, Issue 1, (Part -3),pp.42-48.

[9] J. Hashim, L. Looney and M. S. J. Hashmi, Metal Matrix Composites: Production by the Stir Casting Method, Journal of Materials Processing Technology, 1999, volume. 119, No. 1-3, , pp. 329-335.

[10] Review of Effective Parameters of Stir Casting Process on Metallurgical Properties of Ceramics Particulate Al Composites, IOSR Journal of Mechanical and Civil Engineering (IOSR-JMCE), 2015, volume 12, Issue 6,pp. 22-40.

[11] Mohammed Imran, A.R. Anwar Khan "Characterization of Al-7075 metal matrix composites: a review ''Journal of Materials Research and Technology, 2019, volume 8, Issue 3, pp. 3347-3356.

[12] Yashpal, Sumankantb , C.S.Jawalkarc,Ajay Singh Vermad,N.M.Surie, "Fabrication of Aluminium Metal Matrix Composites with Particulate Reinforcement" Materials Today: Proceedings, volume 4,2017,pp. 2927–2936.

[13] Shanawaz Patil1 , Dr. Mohamed Haneef 2 , Dr. Manjunath L H and Dr. Reddappa H "Investigation on mechanical properties of hybrid graphene and beryl reinforced aluminum 7075 composites" IOP Conf. Series: Materials Science and Engineering 2019,volume 12,pp.577.

[14] M.Vamsi Krishnaa, Anthony.M.Xaviorb, "An Investigation on the Mechanical Properties of Hybrid Metal Matrix Composites" Procedia Engineering, 2014, volume 97, pp. 918 – 924.

[15] B. Ramgopal ReddyC.Srinivas "Fabrication and Characterization of Silicon Carbide and Fly Ash Reinforced Aluminium Metal Matrix Hybrid Composites" Materials today proceedings, 2018,Volume 5, Issue 2, Part 2, pp. 8374-8381.

[16] A. Sathishkumar, R. Soundararajan "Extensive review on properties of metal matrix composites reinforced with Fly ash" International Journal of Mechanical Engineering and Technology (IJMET) Volume 9, Issue 9, September 2018, pp.1219-1231.

[17] Uppada Rama Kantha, Putti Srinivasa Rao b, Mallarapu Gopi Krishnac, "Mechanical behaviour of fly ash/SiC particles reinforced Al-Zn alloy-based metal matrix composites fabricated by stir casting method", Jmaterial research and technology, 2019,8(1), pp-737–744.

[18] Cao Fenghong, Chen Chang, Wang Zhenyu, T. Muthuramalingam & G. Anbuchezhiyan, "Effects of Silicon Carbide and Tungsten Carbide in Aluminium Metal Matrix Composites" 2019, volume11, pp.2625–2632.

[19] Ikubanni Peter P.Oki M. &Adeleke Adekunle A.Blaza Stojanovic, "A review of ceramic/bio-based hybrid reinforced aluminium matrix composites"Journal Cogent Engineering ,volume 7, 2020, Issue 1,pp-1-19.

[20] Rajesh Jesudoss Hynes, R Sankarnarayana, Tharmaraj R,Catalin prucu, "A comparative study of the mechanical and tribological behaviours of different aluminium matrix–ceramic composites", Journal of the Brazilian Society of Mechanical Sciences and Engineering, 2019,volume 41,issue 8,pp.345-356.

ICAMMAS17

Studies on Dry Sliding Wear Characteristics of Cermet WC-Co Particulate Reinforced Al7075 Metal Matrix Composite

Gopal Krishna U B[a],[*], Ranganatha P[a], Rajesh G L[a] Auradi V[a], Mahendra Kumar S[b] and Vasudeva B[a]

[a]R&D Center, Department of Mechanical Engineering, Siddaganga Institute of Technology, Tumakuru,572103,Karnataka, India
[b]R&D Center, Department of Mechanical Engineering, RV College of Engineering, Bengaluru, 560059, Karnataka, India

Abstract

In the present work, an attempt is made to synthesize cermet (WC-Co) reinforced Al7075 metal matrix composite by liquid metallurgy route. The dry sliding wear behavior of these prepared composites was studied with varying sliding speed, load and sliding distance. Cermet in an amount of 6 wt% is used as reinforcement in Al7075 matrix. Microstructural characterization of the prepared composites is carried out using SEM/EDX and XRD studies. X-ray diffraction studies have revealed the peaks corresponding to α-Al, WC, Co and minor Al$_5$W phases. SEM/EDX characterization revealed the uniform distribution of cermets in Al matrix. Dry sliding wear characteristics of the prepared composites were studied using a pin-on-disc testing machine. The wear rate for alloy and composites decreased with increase in sliding speed and increased with increase in applied load and increasing sliding displacement. The worn surfaces of the composites were investigated using optical microscope.

1. Introduction

Metal matrix composites (MMCs) provide improved properties over other monolithic materials, like high strength to weight ratio, high temperature working temperature, wear and corrosion resistance [1]. AMMCs are gaining importance due to light weight and good formability. Al7075 is the type of Al alloy containing Zn and Mg as major alloying elements commonly used for automobile, aerospace and gas cylinders. Al7075 is heat treatable, can be easily welded and good finishing characteristics. Al7075 has high strength among aluminium series and highly corrosive than other aluminium alloy [2]. Particulate composites are widely used due to their low cost and manufacturing ease. Ceramics are commonly used as reinforcements. The reason of metal reinforced with hard ceramic particles provides high strength, wear resistance, stiffness etc [3]. Fabrication of composites is commonly done by stir casting route due to simple, economical and fabrication ease [4, 5]. Eunji Hong *et al.* [6] studied the wear property of copper alloy reinforced with WC. They carried macro and micro level pin-on-disc wear testing analysis.

* Corresponding author. Tel.: +91-9739765392 ; fax: +91-0816-2282994 .
E-mail address: gopalkrishnaub@gmail.com

Wear resistance increases as sliding distance increases in composite compared to copper alloy.Srikanth B G *et al.* [7] carried out investigation on microstructure and tribological behavior of aluminium reinforced with WC and fly ash. Dry slide wear test was carried out. The addition of reinforcements restricts the wear loss due to hard ceramic particulates.

Radhika N *et al.* [8] highlighted on dry sliding wear property of Al/graphite/Alumina of hybrid MMCs. They conducted experiments to evaluate tribological properties like dry sliding behavior by varying load and speed by keeping sliding distance constant. As reinforcement percentage increases gradually, wear resistance also increases and they found wear rate is lower in case of hybrid MMCs compared to unreinforced alloy. Bharath V *et al.* [9] studied on synthesis of 6061Al/Al$_2$O$_3$ composite to evaluate hardness and wear properties. Wear test has been carried out for 6061Al alloy and 6061Al/Al$_2$O$_3$ composite. They found maximum wear loss in matrix compared to composite. Higher wear resistance in composite is achieved due to incorporation of hard ceramic particles into matrix restrict the ploughing action of counter disc, thereby reducing the wear loss of the composite. Rajesh G L *et al.* [10] made comparative study on dry sliding wear behavior of B$_4$C reinforced 6061Al matrix composite. Minimum wear rate is found in composite having 6% volume fraction of reinforcement compared to 4% volume fraction of composite and matrix. This occurs due to formation of protective layer at interface of pin and disc.

Availability of literature on the wear characteristics of cermets reinforced Al composite is very limited. Hence, the present work focuses on processing of Al7075-WC/Co cermet based composite using conventional stir casting technique. Work mainly focuses on studying the wear properties of the prepared composite.

2. Experimental Procedure

2.1 Material selection

The metal matrix material selected for the present study is Al7075 alloy since the mechanical properties can be tailored through heat treatment process and also possesses excellent strength at elevated temperature. The reinforcements were WC-Co cermet of average size 10-15µm of 6wt%. The average density of Al, Tungsten carbide (WC) and Cobalt (Co) were 2.81, 15.63 and 8.9 g/cc respectively. Tungsten carbide being hard and brittle in nature gets accommodated in soft ductile aluminium base matrix, enhancing the overall stiffness and strength of the MMCs. The chemical composition of matrix alloy is given in Table 1.

Table 1. Chemical composition of Al7075 alloy.

Chemical composition	Si	Fe	Cu	Mn	Mg	Cr	Zn	Ti	Al
Wt. %	0.4	0.5	1.6	0.6	2.5	0.15	1.5	0.2	Balance

2.2 Composite preparation

The composite was prepared by stir casting technique. In this method, the Al7075 matrix material was melted at a temperature of 750 °C. The preheated reinforcements were mixed to this matrix material by stainless steel stirrer rotating at 250 rpm to create a vortex, in order to ensure uniform mixing of reinforcements with the molten alloy. Degassing agent C$_2$Cl$_6$ (Hexachloroethane) was added to reduce gas porosities during casting processes. About 1% of Magnesium by weight was added to the molten metal while mixing to obtain good wettability. The molten metal was then poured into a permanent cast iron mould of 120mm x φ15mm dimensions and allowed to solidify. The die was released after 2 minutes and the castings were taken out.

2.3 Wear testing of Composite

A pin-on-disc test apparatus was used to investigate the dry sliding wear characteristics of composite specimens. The specimens were prepared and dry slide wear test was carried out as per ASTM G99 standard in DUCOM pin on disc wear test apparatus. Specimen pins of 10 mm diameter and 30 mm length were machined from the composite bar and then polished metallographically. Each specimen was thoroughly cleaned by acetone solution, dried and then accurately weighed using a single pan electronic weighing machine with an accuracy of 0.0001g. Fig. 1. shows the pin-on-disc apparatus used for wear studies. During the test, the pin was held and pressed on the surface of a hardened EN32 steel disc (60 HRC) by applying load

that act as counter weight and balances the pin. All the specimens followed a same track of 90mm diameter with a tangential force. The LVDT (load cell) on the lever arm helps to determine the wear at any point of time by monitoring the movement of the arm. Once the surface of contact wears out, the load pushes the arm to remain in contact with the disc and the movement of the arm generates a signal. At the end of each test, the specimen was removed, cleaned with acetone to remove any debris and re-weighed to determine the volumetric wear rate. By converting the wear mass loss to wear volumetric loss and dividing by sliding distance, the volumetric wear rate was obtained.

The wear test parameters considered;

- Weight percentage of cermet (6%).

- Applied load (10, 20, 30 and 40 N).
- Sliding speed (0.94, 1.88, 2.82 and 3.75 m/s).
- Sliding distance (250, 500, 750 and 1000 m).

Fig. 1. Schematic view of pin-on-disc dry sliding wear test machine.

3. Results and discussions

3.1 Microstructural characterization

Metallographic test samples sectioned from composite castings are prepared as per metallographic procedure for microstructural analysis. Scanning electron microscopy equipped with EDX (Hitachi Su-1500 model) is employed for identifying presence and distribution of WC-Co cermet particles in Al matrix. The SEM microphotographs of Al7075 matrix and Al7075-WC-Co cermet based composites are presented in Fig. 2(a) and (b) respectively. From Fig. 2(a). it is clear that microstructure of Al7075 matrix consists of α-Al and Si is being distributed at boundaries. Fig. 2(b). representing the microstructure of Al7075-WC-Co cermet based composite reveals fairly uniform distribution of WC-Co cermet particles in an α-Al matrix. Fig. 2(c) and (d) shows energy dispersive x-ray analysis being carried out on Al7075-WC-Co cermet based composite. EDX elemental analysis has shown the peaks corresponding to Al, Mg, W, Co, C, Fe, Si and Ca thus confirming the presence of WC-Co Cermet in Al matrix.

3.2 X-Ray diffraction analysis

XRD is a technique that is widely used in the applications range from phase identification, quantification and determination of crystallite and particle size. Crystallite size can also cause peak broadening. Once the instrument effects have been excluded, the crystallite size is easily calculated as a function of peak intensity, peak position and wavelength. X-ray diffraction (XRD) analysis of the Al7075- 6wt% of WC-Co cermet composite was done using XRD Machine-7000; M/s Shimadzu Analytical India Pvt. Ltd. and is presented in Fig. 3. The 2θ range was selected such that all the major intense peaks of the phases expected were covered.
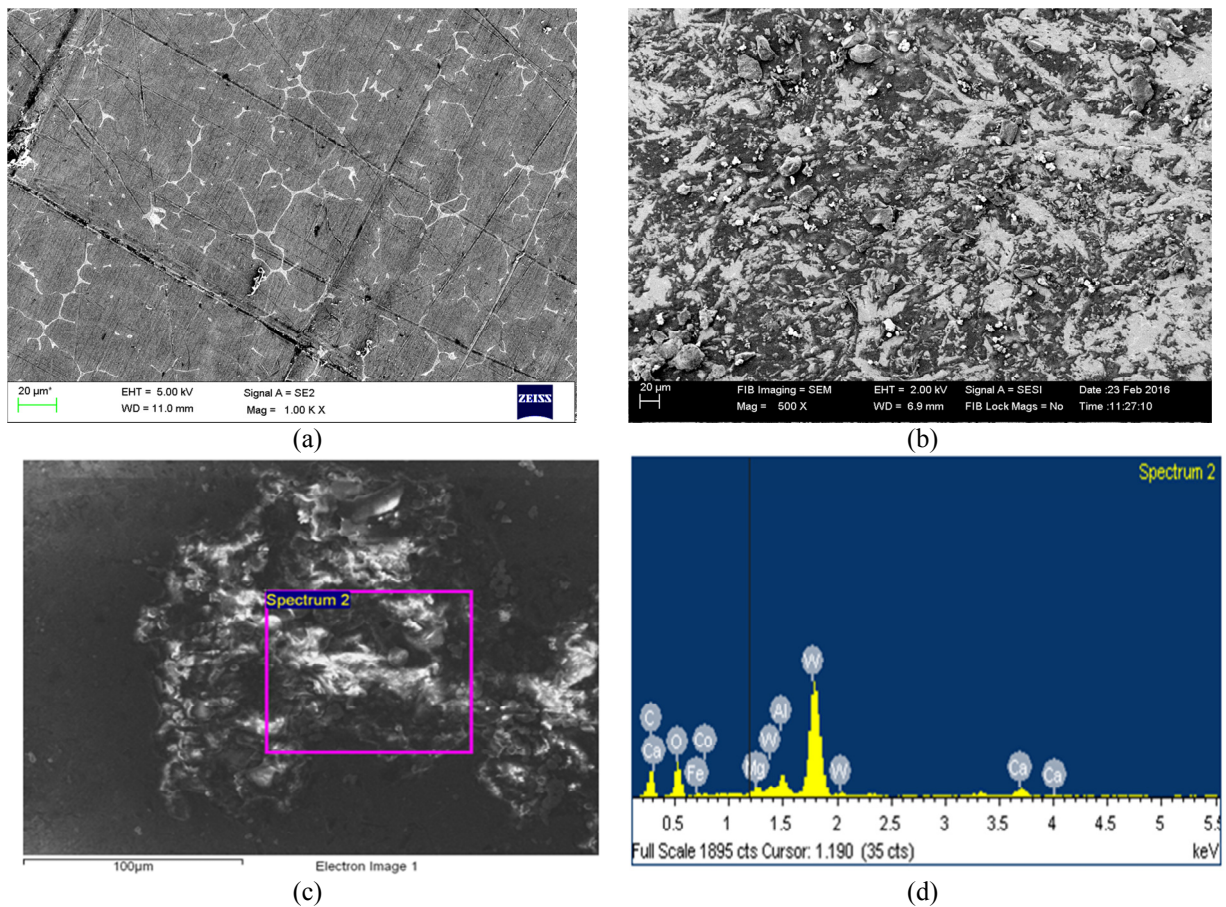
Fig. 2. Shows SEM microphotographs of (a) Al7075 matrix (b) Al7075- 6wt% of WC-Co cermet composite produced at 750 °C by stir casting (c) region for EDX spectrum (d) EDX spectrum of Al7075- 6wt% of WC-Co cermet composite.

Analysis of the XRD pattern shows the peaks corresponding to major phases of Al, WC, Co and minor phases of Al_5W. Probably the Al_5W phase might have been formed at the interface by the reaction between Al matrix and WC-Co cermet particles. Therefore, detailed interfacial studies are necessary in order to fully understand the chemical interaction products formed at the Al7075 and WC-Co cermet interface.

3.3 Effect of sliding velocity on wear rate

The variations in the wear rate of the matrix and the cermet reinforced composite under varying sliding velocities of 0.94, 1.88, 2.82 and 3.75 m/sec at constant load of 19.62N and sliding distance of 500m are as shown in Fig. 4. Wear rate of the matrix alloy and composite decreases with increase in sliding velocity from 0.94-3.75 m/sec. Wear resistance is higher in Al7075-WC-Co composite compared with matrix alloy. This is mainly due to mechanically mixed layers like oxide layers and worn-out debris acts as lubricating materials between disc and specimen. At higher speed contact surface may get reduced and due to increase in temperature localised surface of the material may become smoother, promote yielding and cause abrasive wear to delamination of the wear surface. Hence, the WC-Co composite have more wear resistance than unreinforced alloy.
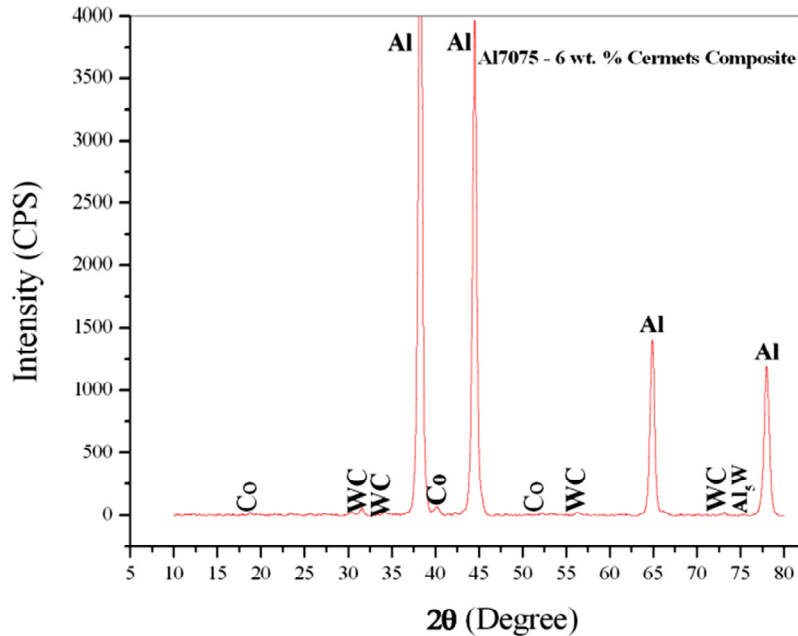
Fig. 3. Shows X-ray diffraction pattern of Al7075-6wt% of WC-Co cermet composite prepared at 750°C using melt stirring method.
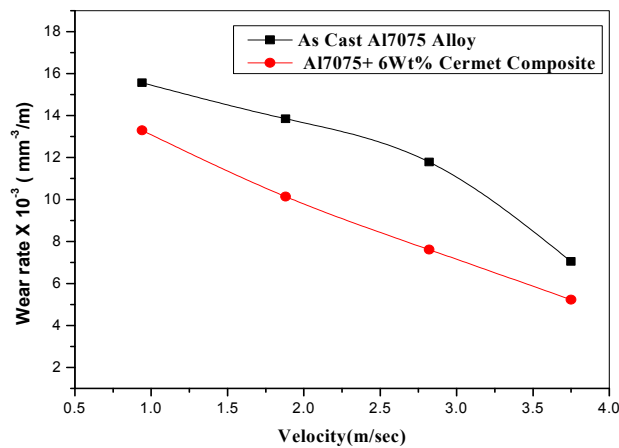

Fig. 4. Variations in wear rate of Al7075 matrix and cermet reinforced composite under varying sliding velocity at constant load of 19.62N and at constant sliding distance of 500m.

3.4 Effect of varying load on wear rate

The variations in the wear rate of the matrix and the cermet reinforced composite under different loading condition with constant sliding distance and velocity of 500m and 1.88m/s are as shown in Fig. 5. It is clear from the figure that addition of WC and Co particles results in lesser wear rate when compared to unreinforced alloy at all loads. With increase in load, pressure at the pin-on-disc interface becomes more. At lower load, wear rate is less. As load increase gradually wear rate goes on increasing. Since, Al is a softer material undergoes adhesive wear resulting in higher wear rate in Al7075 alloy. Presence of hard ceramic particles WC and Co particles in the prepared composite will resist the pressure applied and also bonding between Al, WC and Co particles avoids the loss of material from the contact surface leading to abrasive wear with reduction of wear rate.
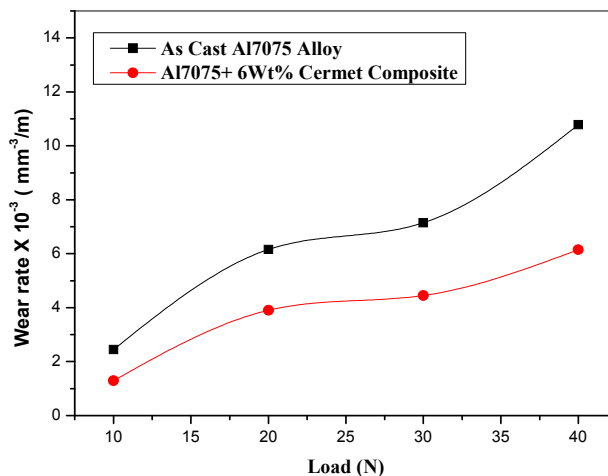
Fig. 5. Variations in wear rate of Al7075 matrix and cermet reinforced composite under varying loading conditions at constant sliding velocity of 1.88m/s and constant sliding distance 500m.

3.5 Varying sliding distance

The variations in the wear rate of the matrix and the cermet reinforced composite under varying sliding distance at constant load and sliding distance of 19.38N and 1.88m/sec are as shown in Fig. 6. It clearly indicates, the addition of WC-Co particles to Al7075 alloy has resulted in lesser wear rate when compared to the unreinforced Al7075 at all varying sliding distance.
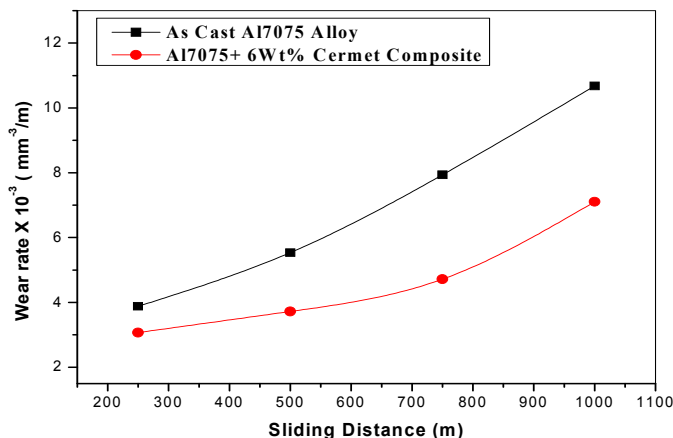

Fig. 6. Variations in wear rate of Al7075 matrix and cermet reinforced composite under varying sliding distance at constant load of 19.38N and at constant sliding velocity 1.88m/sec.

As sliding distance increases wear rate also increases due to thermal softening of contact surface. At higher sliding distance temperature is more due to longer time of contact between the specimen and disc due to which localised heating occurs at the contact surface. Wear resistance is more in Al7075-WC-Co composite due to the presence of hard ceramic particles of WC protect from high temperature effect. As temperature increases at the longer sliding distance forms oxide layer due to oxidation of aluminium alloy matrix, which acts as a lubricating medium prevents wear rate in composites.

Worn surface studies shallow and deep grooves and surface delamination indicating adhesive wear. Addition of WC-Co particles to Study of worn surfaces of Al7075 alloy and prepared composite were carried out after dry sliding wear test using optical microscope. It is clear from micrograph (Figures 7(a) and (b)) that unreinforced Al7075 alloy has shown large surface cracks Al7075 alloy resulted in decrease in wear loss when compared to matrix. It is clearly evident from the worn surface images in Fig. 7(c-d). addition of particulates result in few smaller cracks and oxide formation on the wear surface. From the worn surface examination it is

clear that unreinforced Al7075 alloy have shown more wear rate resulting from the plastic deformation of matrix material.
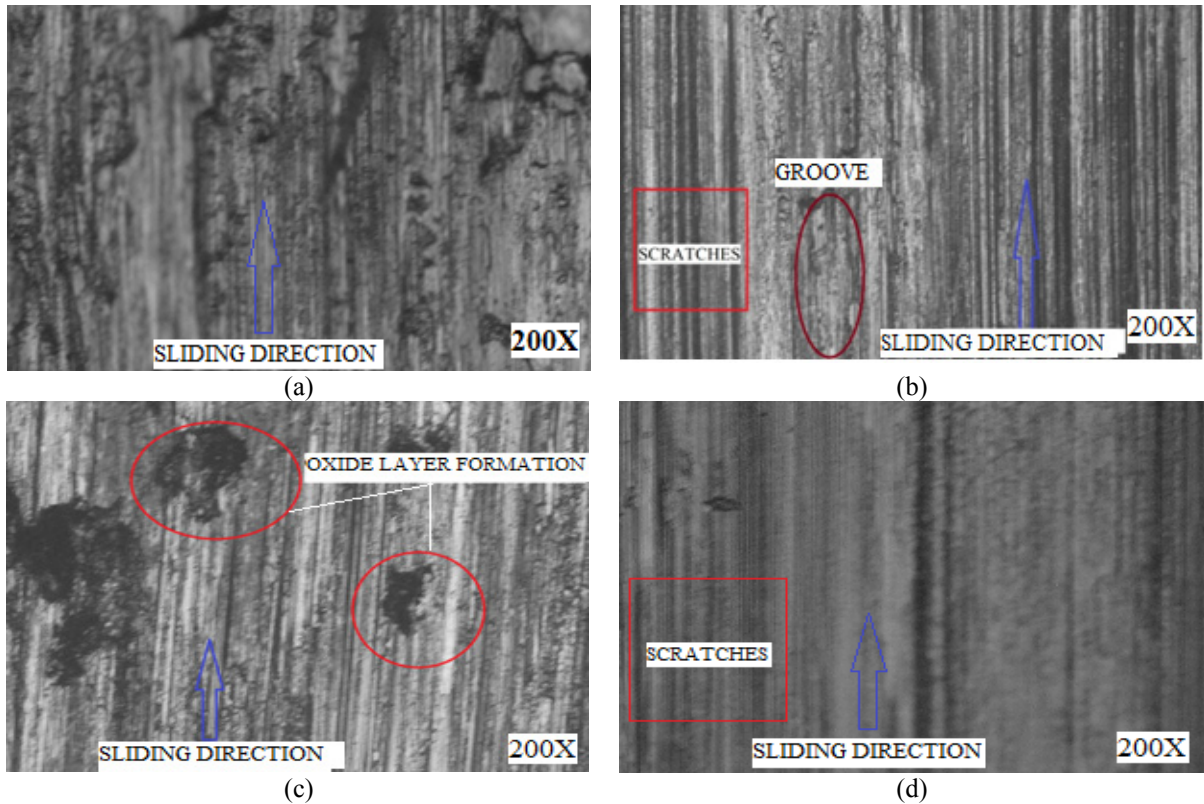
3.6

Fig. 7(a-d). Shows the optical micrographs of as cast Al7075 and WC-Co cermet composite at 200X after wear test, (a-b) as cast Al7075, (c-d) with 6wt% of WC-Co cermet composite.

Wear rate reduction is mainly due to the formation of mechanically mixed layers. It acts as a lubricating material between the rotating steel disc and specimen and plays an important role in keeping the wear rate low. From Fig. 3.6 (d) it is observed that the width of the grooves and scratches reduce with addition reinforcement. This is due to the resistance offered by the particulates to the wear of the specimen. At higher loads and at higher speeds more scratches and grooves were observed. This shows the characteristics of abrasive wear. Fig. 7(c-d). abrasive wear is observed in the prepared composite, which is mainly due to hard WC particulate present on the wear surface. As WC-Co particles restrict the delamination process, the wear resistance is higher in case of Al7075-cermet composites.

4. Conclusions

Studies on dry sliding wear properties of Al7075-6wt% WC-Co cermet based composite prepared by stir casting route has led to the following conclusions.

- Al7075-6wt% WC-Co cermet based composite was successfully synthesized by conventional stir casting technique.
- Microstructural characterizations carried out using SEM studies have revealed fairly uniform distribution of the WC-Co cermet particles in the Al7075 matrix system.

- X- ray diffraction analysis has revealed the presence of major phase of Al, WC, Co and minor phase of Al_5W.
- The wear rate of MMCs and alloy has increased with increase in applied load, sliding distance and decreased with increase in sliding speed.
- The wear rate of cermet reinforced composite is lower than the unreinforced Al7075 alloy in all applied conditions.
- Optical micrographs of wear samples showed minimum ploughing and minimum groove formation in cermet reinforced composite when compared with Al7075 alloy without reinforcement.

References

[1]   Hartaj singh, Sarabjit, J. Eng. Res. Stud. 2 (2011) 72-78.
[2]   U.B. Gopal Krishna, P. Ranganatha, V. Auradi, S. Mahendra kumar, B. Vasudeva, Mater. Sci. Eng. 149 (2016) 1-8.
[3]   C.S. Ramesh, R. Keshavamurthy, B.H. Channabasappa, Abrar Amhed, Mater. Sci. Eng. A. 502 (2009) 99-106.
[4]   Hari Prasada, Balamurugan, A. Adhithan, Syed Bava Bakrudeen, Int. J. Soft. Comput. Eng. 2 (2013) 257-261.
[5]   A. Sato, R. Mehrabian, Metall. Trans. B. 7 (1976) 443-451.
[6]   Eunji Honga, Bradley Kaplin, Taehoon You, Min-Suhab, Yong-Suk Kima, Heeman Choea, Wear. 270 (2011) 591–597.
[7]   G. Amarnath, B.G. Srikanth, Int. J. Res. Eng. Technol. 4 (2015) 567-572.
[8]   N. Radhika, R. Subramanian, S. Venkat Prasat, B. Anandavel, Ind. Lubr. Tribol. 64 (2012) 359–366.
[9]   V. Bharath., Madev Nagaral, V. Auradi, S. A. Kori, Procedia. Mater. Sci. 6 (2014) 1658 – 1667.
[10] G. L. Rajesh, V. Auradi, Umashankar, S. A. Kori, Procedia. Mater. Sci. 5 (2014) 289 – 2

The wear properties of ceramic B$_4$C/Al matrix composite at elevated temperature under dry sliding

Rajesh Gandasi Lakshmikantha, Soundarya Nanjundaswamy, Thilak Kumar Jayaprakash, Rohan Kundwada Ravindra, and Virupaxi Auradi

View Online   Export Citation

ARTICLES YOU MAY BE INTERESTED IN

The Wear Properties of Ceramic B$_4$C/Al Matrix Composite at Elevated Temperature under Dry Sliding

Rajesh Gandasi Lakshmikantha[1, a)] Soundarya Nanjundaswamy[1, b)] Thilak Kumar Jayaprakash[1, c)] Rohan Kundwada Ravindra[1, d)] and Virupaxi Auradi[1, e)]

[1]R & D Centre, DME, Siddaganga Institute of Technology, Tumakuru 572103 Karnataka India.

a)Corresponding author: rajeshkanth2010@gmail.com
b)soundaryanswamy@gmail.com c)thilakmandya@gmail.com d)rohan.kr8@gmail.com e)vsauradi@gmail.com

Abstract. Ceramic B$_4$C particulates with an average particle size of 33 μm were reinforced with 6061Al matrix by novel two step melt stirring at 750°C. In experimentation, an addition level of 7Wt% B$_4$C$_p$ and K$_2$TiF$_6$ flux is ball milled to achieve 0.15 ratios for 2hours. The B$_4$C particulate composites were characterized and tested for hardness and wear properties evaluation. Scanning Electron Microscopy (SEM) micrographs have fairly dispersed ceramic B$_4$C particulates with in ductile Al matrix attributed to two-step process and K$_2$TiF$_6$ flux. Dry sliding wear behavior of prepared ceramic composite were measured by Pin-on-disc wear evaluating apparatus at 200°C test temperature under atmospheric humidity condition. Results showed that pull-out of B$_4$C$_p$, formation of tribo-film and oxidation of Al protects the direct contact of composite pin at interface under room temperature condition whereas at elevated temperature, composite pin suffer severe plastic deformation due to temperature assisted diffusion of Al atoms; thereby decreasing the wear performance of ceramic composite at all loads. /Energy Dispersive X-ray Spectrometry (EDS) were used to identify the type of wear mechanisms and to understand the surface morphology.

Keywords: Ceramics, Elevated Properties, Surface Morphology, Pin-On-Disk.

INTRODUCTION

Nowadays aluminum metal matrix composites have got their own priority in sectors like aerospace, automobile, chemical transportation etc. Because of their high energy to mass ratio, improved wear opposition & high elastic modulus makes them more suitable to use in some special purpose applications like space shuttle engine components, missile guidance system etc. [1]. B$_4$C is the third hardest (3700 N/mm^2) material known after cubic boron nitride and diamond, with low density value of 2.52g/cc and B$_4$C has got very good thermal conductivity property to strengthen Al alloy matrix[2,3]. Many research work has been carried out on 6061Al-B$_4$C$_p$ composites, it is difficult to mix B$_4$C particles in Al melt, uniformity and good wettability of B$_4$C particles can be achieved with the help of halide salt (K$_2$TiF$_6$) [4,5]. Wear studies on 6061Al-B$_4$C$_p$ composites is very limited. Generally incorporation of hard particles inside soft material increases the wear resistance as hardness and surface roughness of material increases.

In present study, 6061Al alloy metal matrix is incorporated with B$_4$C$_p$ particulates size of 33 microns with volume fraction of 7 wt. % at 750°C to produce aluminum matrix composites by two stage stir casting method. K$_2$TiF$_6$ flux added to melt for proper bonding between 6061Al and B$_4$C$_p$ particles; flux which reacts exothermically inside melt and improves wettability. Uniformity of reinforcements (B$_4$C) in matrix can be accomplished by superior stirring action. Wear under dry condition was analyzed with pin-on-disc, shifting the parameters - load, sliding distance & sliding velocities under room and elevated temperatures (200°C). Using SEM/EDS the worn surfaces of specimens were studied.

EXPERIMENTAL DETAILS

7wt. % of B_4C particulates (particle diameter 33 microns) reinforced in 6061Al alloy composites were produced by melt casting technique. Flux (K_2TiF_6 with 0.15 Ti/ B_4C ratio) was used to increase wettability between 6061Alalloy and B_4C particles [2, 6]. Specimens were prepared using mold of cast iron having 125mm length and 15mm diameter. 500 grams of Al alloy was charged to crucible (clay graphite) and using resistance furnace the charge was melted. Cover flux were added to decreases the contact angle and surface tension forces [2]. C_2Cl_6 degassing agent (hexochloroethane) was used to remove the gasses, those adsorbed in the melt aluminum. The stirring was carried out for 5min using zirconia coated steel rod for the generation of vortex. Then the mixture of K_2TiF_6 and B_4C particulates were added to the melt at 750°C temperature. Instead of adding the mixture all at once, it's divided in two stages equally and then added with continuous feed rate to get uniform spreading throughout the specimen. Two stage additions of particle mixtures avoid the cluster formation among B_4C particulates. At 750°C, 6061Al reinforced with B_4C_p composite was poured in to a pre-heated mold and after holding for about 1 minute, the specimens were taken out. From prepared castings the metallographic test samples were prepared to study microstructures of composite. SEM and EDS were employed to check uniformity of B_4C particles in Al matrix and to confirm B_4C presence in matrix respectively. Rule of mixture and Archimedes principle were employed to measure densities theoretically and experimentally. Zwick micro-Vickers hardness test machine was employed to measure hardness of composites as well as aluminum matrix on polished specimen surface under 2N load with 10 sec dwell time. At 20 different locations an average value of 40 readings were taken. Wear investigation under dry sliding was measured by pin-on-disc machine. The wear samples (pin) were prepared according to ASTM G99 standards (30mm length and 8mm diameter). The counter face material used against samples was spinning S.S disc of 63 HRC with track diameter of 90 mm. Pin surfaces were slide against disc by means of emery sheet of 85 grit size. After every sample trial, the pins as well as disc were scrubbed through acetone & they were weighed using electrical weighing machine with 0.002 grams accuracy. For elevated temperature tests, the pin holding knob was fixed on to arm and temperature was adjusted to 200°C and above procedure of wear test was repeated. The test parameters considered were load, sliding distance and sliding velocity. Normal load selected - 9.81N to 39.24N with maintaining sliding distance 499.98 m along with sliding velocity of 1.879m/s invariable. Then the sliding distance and sliding velocities were varied from 250 m to 1000 m and 0.94 m/s to 3.76 m/s by keeping constant load of 19.619 N respectively.

EXPERIMENT OUTCOME AND DISCUSSIONS
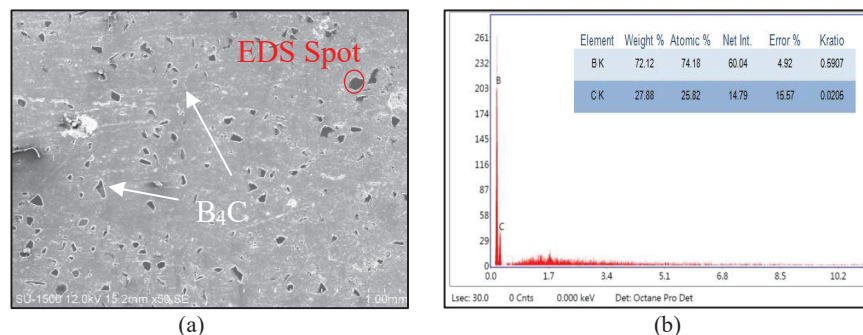
Characterization and Property Evaluation

(a)   (b)

FIGURE 1. SEM micrograph of (a-b) 6061Al-7wt. % B_4C_p composite with EDS analysis

Figure.1 (a) discloses that the distribution of B_4C_p in the Al matrix is moderately consistent. Addition of K_2TiF_6 flux has led to superior stretch of the Al matrix on the exterior of B_4C particle at pour temperature of 750°C. It is assumed that the existence of titanium in the form of K_2TiF_6 flux contribute headed for elimination of the oxide coat from Al melt, thus convalescing the wettability. In count, the stirring has altered effect on the microstructure of the composite as seen in Fig. 1(a). SEM micro images have also discovered the occurrence of the Titanium deposit adjoining boron carbide particles. In mandate to authorize the existence of Ti coat, EDS examination were conceded out at the perimeter of the B_4C_p which is adhere in the form of pale coat adjoining B_4C_p (Fig. 1(b)).

Ti coat was designed at the point of adding K_2TiF_6 into the matrix with B_4C_p. The K_2TiF_6 flux will go through an exothermic reaction when make contact with fluid Al matrix. Since reaction is spirited and exothermic in nature which lead to creation of the Al_3Ti coat ensuing superior bonding nature. The physical properties & hardness (Micro Testing) of the composites are analyzed and are reported in Table 1. From above table it is understandable that adding of B_4C_p to 6061Al matrix lessens density & improves hardness of the 6061Al. Hardness of a soft material increases when hard particles incorporate them and it prevents material from plastic deformation [9, 2]. Grain size of material decreases during solidification as hard particles inside molten metal provides extra heterogeneous nucleating sites. This results in hardness enhancement in a material. Density of prepared composite is fewer that of aluminum matrix; B_4C has density of 2.52 g/cc. B_4C particulates were mixed with help of flux allowing more amount of B_4C_p to mix with melt, in doing so, reducing the density of the Al/Boron carbide composite [4]. The observed porosity of composite can be due to aspects like pour timing, shrinkage, gas trap in melt, H-evaluation etc. [10, 4].

TABLE 1. Physical properties and hardness of 6061Al alloy & 6061Al with 7 weight fraction of B_4C composite

Nominal composition	Theoretical ρ (g/cc)	Experimental ρ (g/cc)	% Porosity	Micro hardness (VHN)
6061Al	2.70	2.6744	0.94	70.34
6061Al-B_4C (7wt. %)	2.6874	2.6147	2.70	146.36

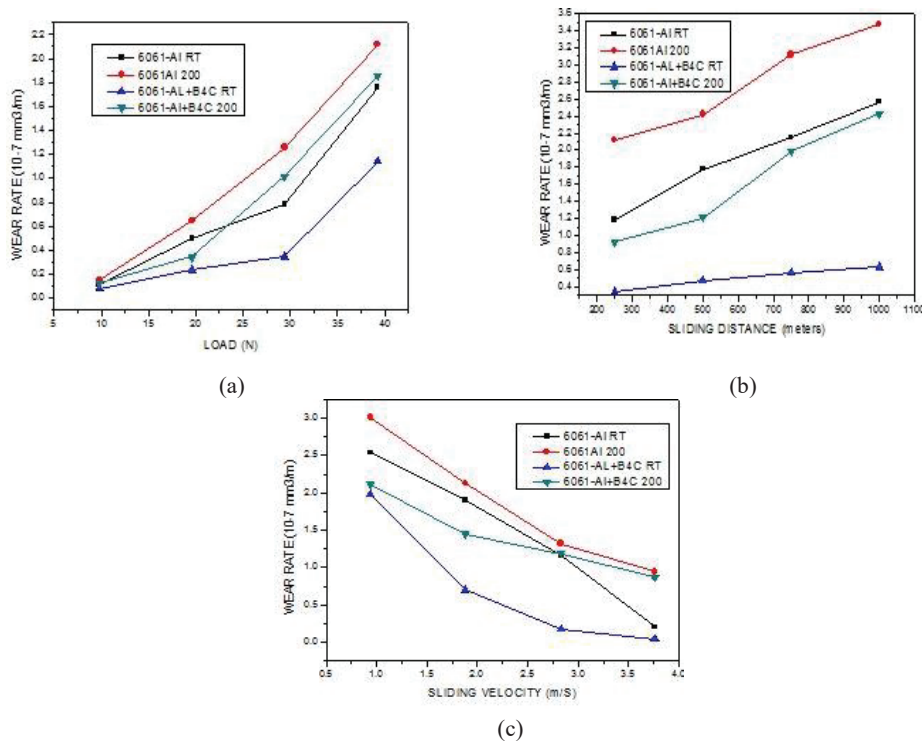## Wear Studies

(a)

(b)

(c)

FIGURE 2. Influence of (a) Load; (b) sliding distance (c) Sliding velocity on as cast 6061Al alloy and 6061Al-B_4C_p composite tested at Room temperature and 200°C respectively.

Room and elevated temperature wear behavior of unreinforced 6061Al alloy as well as 6061Al-B_4C_p composites were studied and results of the same are presented in Fig. 2. From graph it is evident that the wear rate of both Al matrix and composite (6061Al-7wt. % B_4C_p) boost with raise in applied load. In case of composite incorporated B_4C particles does not allow matrix material to come in contact with counter face material at some portions. Hence reduces the wear rate when compared to base metal matrix. Increase in load, increases metal deformation rate and time necessary for changeover from gentle wear to severe wear decreases, that's why the wear rate amplifies [11].

Sliding distance is directly proportional to sliding time. As time increases the contact linking sample & disc also increases, when contact time enhance the heat creation velocity will be more, this direct to higher plastic deformation which causes more matter removal rate thus wear resistance is reduced.
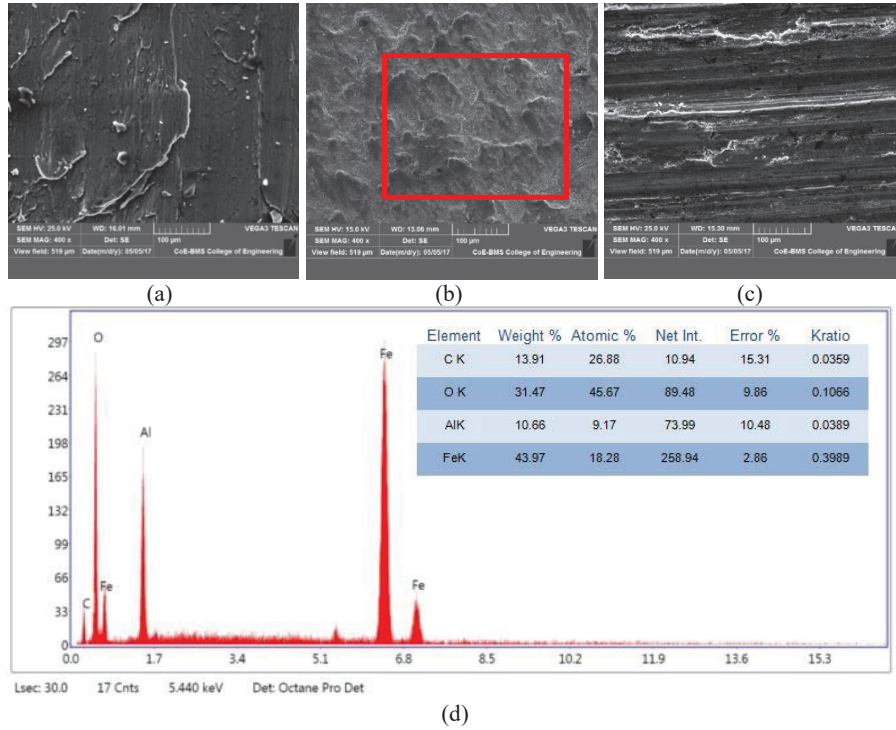

(a)   (b)   (c)

Element	Weight %	Atomic %	Net Int.	Error %	Kratio
C K	13.91	26.88	10.94	15.31	0.0359
O K	31.47	45.67	89.48	9.86	0.1066
AlK	10.66	9.17	73.99	10.48	0.0389
FeK	43.97	18.28	258.94	2.86	0.3989

Lsec: 30.0   17 Cnts   5.440 keV   Det: Octane Pro Det

(d)

FIGURE 3. SEM image showing worn surfaces of (a) 6061Al alloy (b-c) 6061Al- B_4C_p composites at 200°C sliding at velocity of 1.879 m/s with load 19.619 N for sliding distance of 499.98 m respectively (d) EDS results showing Fe and O peaks, which confirms adhesion of iron from disc to pin material.

Sliding velocity is inversely proportion to time as presented in Fig. 2(c). The contact time between pin and the counter face disc decreases as sliding velocity increases there by reducing the metal removal rate of pin. So as sliding velocity increases wear rate decreases. At higher load and speed material shows more wear rate due to subsurface deformation and cracks [12], so sometimes wear rate increases with sliding speed also.7wt. % volume fraction addition of B_4C particles in 6061Al matrix shows abrasive wear mechanism where 6061Al alloy shows adhesive wear mechanism as shown in Fig. 3(a-c). Further, Fig. 3(a-c) also reveals that two body and three body abrasions (mixed wear mechanisms) are found here mainly because of micro-plough which has resulted bulky face grooves, tough particles pulled away from matrix between counter face material and pin causes wear debris. Composites shows small surface cracks, mild patches, and smaller grooves when compared to base material. Three body abrasion wear was observed in case of the composite materials. Tribolayer created at a point of sliding, act as shield against added abrasion of material from surface, this layer does not allow Pin-disc contact and results in lesser wear rate [12].

At 200°C, 19.619 N load with nominal velocity (1.879 m/s) the disc (Stainless steel) material undergone wear, material from disc, stick to surface of sample and it is confirmed by EDS analysis exposed in Fig.3(d); i.e. iron elements present in steel disc were adhered to pin surface. This shows that hard particles of boron carbide increases wear resistance of matrix material. But at some portions of pin due to high heating effect (increase in temperature) thermal softening of material takes place and leads it to more plastic deformation which results in higher wear. Though the wear rate at 200°C is more in composites, it is very less compared to that of 6061Al alloy. The wear mechanism was greatly influenced by hard boron particles inside the Al matrix. B_4C particles offer resistance to the wear during sliding.

CONCLUSION

In present study, 6061Al reinforced with B_4C_p composites was produced at 750°C using stir casting technique. Wear properties of prepared composites and 6061Al alloy were studied at both room temperature and 200°C by varying load, sliding distance, sliding velocities. Worn surface study was done using SEM photographs of samples. Conclusions of present work are as follows:

- K_2TiF_6 with 0.15 ratio has improved the bonding between B_4C and Al alloy matrix at low temperature value of 750°C and uniform distribution of B_4C observed which is clear from SEM images.
- Density of composite material was found lower (2.61 g/cc) compared to matrix material. % porosity has advance from 0.94 (6061Al matrix) to 2.70 by inserting 7wt. % V_f of B_4C_p. Hardness of 6061Al matrix alloy has improved from 70.34 VHN to 146.36 VHN by addition of B_4C_p.
- Boron carbide particles along with Al matrix produces oxide coat (tribolayer) which resist further plastic deformation resulting in lower wear rate.
- At both room temperature and 200°C composites (6061Al-7wt. % B_4C_p) shows lower wear rate compared to 6061Al matrix. At high temperature (200°C), 1.88m/s sliding velocity and 500 meters distance the material show more wear resistance and abrasion of counter face material was observed which indicates oxide formation by Fe and O, this was confirmed by EDS pattern.

ACKNOWLEDGEMENTS

REFERENCES

1. M. Balasubramanian, *Composite Materials and Processing* (CRC press Taylor & Francis group, Boca Raton 2013), pp. 6-15.
2. G. L. Rajesh, V. Auradi, Umashankar and S. A. Kori, Procedia. Mater. Sci **5**, 289-294 (2014).
3. V.A. Katkar, G. Gunasekaran, A. G. Rao and P. M. Koli, Corros. Sci **53(9)**, 2700-2712 (2011).
4. V. Auradi, G. L. Rajesh and S. A. Kori, Procedia. Mater. Sci **6**, 1068-1076 (2014).
5. K. Kalaiselvan, N. Murugan and Siva Parameswaran, Mater. & Des **33**, 4004-4009 (2011).
6. I. Kerti and F. Toptan, Mater. Letters **62(8-9)**, 1215-1218 (2008).
7. V. Auradi, G. L. Rajesh, and S. A. Kori, Mater. & Manuf. Processes **29(2)**, 194-200 (2014).
8. Ping Shen, Binglin Zou, Shenbao Jin and Qichuan Jiang, Mater. Sci. Eng. A **454-455**, 300-309 (2007).
9. C. S. Ramesh, R. Keshavamurthy, B. H. Channabasappa and Abrar Ahmed, Mater. Sci. Eng. A **502(1-2)**, 99-106 (2009).
10. J. Hasim, L. Looney and M. S. J. Hashmi, J. Mater. Process. Technol **92-93**, 1-7 (1999).
11. B. C. Majumdar, *Introduction to Tribology of Bearings* (A. H. Wheeler & co. Pvt ltd, Allahabad India 1986), pp. 77-85.
12. M. Uthayakumar, S. Aravindan and K. Rajkumar, Mater. & Des **47**, 456–464 (2013).

Processing and evaluation of Al/B$_4$C particulate MMC's: Tensile strength and wear properties under different elevated temperature test condition

Rajesh Gandasi Lakshmikantha *, Virupaxi Auradi

R and D Centre, Department of Mechanical Engineering, Siddaganga Institute of Technology, B.H Road, Tumakuru 572102, Karnataka, India

ARTICLE INFO

ABSTRACT

In the present investigation, preheated K$_2$TiF$_6$ flux were blended with B$_4$C particle (an average size of 33 μm) at 0.2 ratios and were incorporated into molten Al at 750 °C through conventional stir casting. Microstructural studies of as cast 6xxx alloy and composite were done using SEM/EDS/XRD. A fairly uniform distribution of B$_4$C particles were observed throughout the matrix with few agglomeration at certain places. Ultimate tensile strength and wear behaviour of the prepared composite were tested using computer assisted UTM and Pin-On-Disk apparatus under elevated temperature (100 °C and 200 °C) respectively. The results shows that strength of composite decreases under the influence of temperature at all testing parameters. It is believed that material had undergone severe plastic deformation before the initiation of necking and mild brittle to severe ductile transition has occurred leading to catastrophic failure at high temperature and is evident from the fractography studies. The formation of tribo-coat or layer at the Pin sample and steel disc interface restricted the direct contact with each other. Further, the addition level of test temperature and developed frictional heat encourages Al atoms to diffuse faster at the slip plane resulting in severe wear from the material surface. Small narrow abrasive lines, particle debonding, softened tribolayer along with few wear debris adhered to worn surface (due to micro ploughing and oxidation) were observed on the surface of composite at all conditions under 200 °C test temperatures. Presence of "O" and "Fe" peak in the EDS pattern (on worn surface) confirms the existence of oxidation layer and micro ploughing on steel disc at higher test temperature.

© 2019 Elsevier Ltd. All rights reserved.
Selection and peer-review under responsibility of the scientific committee of the 2nd International Conference on Recent Advances in Materials & Manufacturing Technologies.

1. Introduction

Aluminum, as a matrix material in metal matrix composite were extensively utilized because of its age hardening nature; less denser, can be easily fabricated and noble engineering features. Among the other Al alloys, heat treatable 6061aluminum (6061Al) has been comprehensively opted in the region of construction, automotive, and marine fields due to high corrosion resistance with moderate strength. Boron carbide particulates (B$_4$C$_P$); being good chemical and thermally stable, low density and higher hardness compared to Al$_2$O$_3$ and SiC [1,2] mark it to use as reinforcement material. Lee et al. [3] discussed the influence of reinforcement type on the tensile strength of the Al/B$_4$C$_P$ and

Al/SiC system and concluded that strength of Al/B$_4$C$_P$ composites is superior to that of the Al/SiC composites at room temperature.

Halverson et al. [4] conveyed that the processing difficulties and mechanical property restrictions can be decreased by incorporation of B$_4$C$_P$ cermet. The addition of degassing capsules (about 4 g) reduced the porosity which in turn advance the tensile strength. K$_2$TiF$_6$ flux addition develops good bonding behavior of B$_4$C$_P$ with 6061Al. Kennedy and Brampton [5] proposed that, control of the interfacial reaction at 6061Al/B$_4$C$_P$ interface, apart from wetting, is also essential in the fabrication of 6061Al/B$_4$C$_P$ composites. The tensile strength of a composite material be influenced by particle homogeneity, gauge length, particle size, and chemical alignment of matrix material. Further, a dependency of tensile failure on the scattering of reinforcement (chiefly clustering and particle dimension) has been witnessed [6–9]. The authors Ho and Lavernia [10] explained the potential strengthening mechanisms operating in particle-reinforced aluminum matrix composites

(AMCs) are: (a) Orowan strengthening; (b) Grain and substructure strengthening, which outcome from the dislocations caused to accommodate the differential thermal shrinkage between the reinforcing particles and the matrix; and (c) Work hardening, which rises due to the strain misfit among the elastic reinforcing particles and the plastic matrix. Maniatty et al. [11], perceived that increase in test temperature, permits further slip systems to function in AMC's allowing general plastic deformation to arise former to the failure. Majumdar [12], in his findings, reported that composite with B_4C particles will not allow Al matrix to come in interaction with counter surface at some portions during sliding thereby moderates the wear rate compared to Al matrix alone. Increase in the applied load, enhances the metal deformation rate and time essential for substitution from tender wear to severe wear decreases, that's why the wear rate intensifies. 3 body abrasion wear was witnessed by Uthayakumar et al. [13] in AMMC's. Tribolayer formed at a point of sliding, act as guard against additional abrasion of material from surface, this layer does not permit Pin-disc contact and results in lesser wear rate at the room temperature as well as high temperature test condition. In detail experimentation is mandatory to realize the impact of test temperature on tensile and wear property of Al reinforced composite. In the present work, Al/B_4C composite were synthesized via conventional stir casting at 750 °C. UTS and wear property of the prepared composite were tested using computer assisted UTM and Pin-On-Disk apparatus under test temperature of 100 °C and 200 °C respectively. Finally, fractography and surface morphology of tested composites were co-related towards conduct of deformation and abrasion.

2. Composite fabrication and testing parameters

Boron carbide reinforced 6061Al matrix composites having 11 wt% of B_4C_P were made by stir casting route using two step addition level of B_4C. A blend of B_4C_P with typical particulate size of 33 μm and K_2TiF_6 (0.2 ratio) was preheated to 250 °C in a muffle furnace. The necessary volume of B_4C_P and K_2TiF_6 were weighed and dry mixed in a pot mill for 30 min using ceramic grinding media. As described in past studies [14,15] to accomplish 100% yield at and above 800 °C, Ti to B_4C ratio should at least be 0.07. In the current work, a temperature of 750 °C was opted to synthesis Al/B_4C composite; therefore, we used Ti to B_4C weight ratio of 0.2. For the composite preparation, 6061Al was liquefied in resistance furnace at 750 °C. The heat was precise within an accuracy of ± 5 °C with aid of digital temperature control. The preheated blend of B_4C_P + K_2TiF_6 (0.2 ratio) were added in two steps into melted 6061Al alloy and stirred by an axial stream S.S impeller at 350 rpm for about 5 min, since high speed rotation (forceful for shorter period of time) ensued in vortex creation. Cover flux with 45% NaCl + 45% KCl + 10% NaF were added earlier to B_4C and K_2TiF_6 to shield the melt from atmospheric oxidation. Further, in order to evade corrosion of the steel impeller, a thin layer of Zr paste was applied and preheated at 300 °C for 45 min in an electric oven. Upon vigorous stirring, the mix was poured into a preheated metallic mold made of cast iron material.

Microstructural characterization: The specimens were cut into cylindrical shape (12.5 mm diameter and 15 mm length) from the central part and polished via different grit size papers of 220, 400, 600, 800 and 1000 μm sequentially using Metallurgical specimen polishing machine. The samples were again polished on velvet material with kerosene as coolant and then etched by Keller's reagent – 2.5% HNO_3, 1% HF, 1.5% HCl and 95% H_2O to advance the contrast. Scanning electron microscopy (SEM) furnished with energy dispersive X-ray spectroscopy analysis (EDS) (Hitachi Su-1500 model) were used to pinpoint the morphology and dispersal of B_4C_P in Al matrix. X-ray powder diffraction (XRD) analysis; to

determine the elemental phases formed during the composite casting, through XRD Machine-7000; M/s Shimadzu Analytical India Pvt. Ltd. Rule of mixture and Archimedes principle were adopted to measure both theoretical and experimental density.

Property Testing: Zwick micro-Vickers hardness test machine was used to determine the overall hardness of composite; should be mirror polished surface, under 2 N normal load for 10 sec dwell time. At 05 different localities, an average value of 20 readings (VHN) were noted. Uniaxial tensile test of Al/B_4C composite were conducted using an INSTRON 8801 tensile testing machine.

The tensile property extents monitored the measures outlined as per ASTM E8M with a crosshead testing speed of 3 mm min-1 for the test samples. The tests were performed on three specimens for both under 100 °C and 200 °C condition respectively and an average value were documented. Wear examination under dry sliding was measured by computer assisted pin-on-disc machine at moderate humidity conditions. The wear samples (pin) were prepared according to ASTM G99 standards – 8 mm diameter and 30 mm length. The counter face material against samples was S.S disc of 63 HRC with track diameter of 90 mm. The test parameters considered were normal load, sliding distance and sliding velocity. Normal load ranging from 9.81 N to 39.24 N was applied on the cast pin maintaining the sliding distance of 500 m and sliding velocity of 1.879 m/s unchanging. After each trial, the pin as well as disc were scrubbed through acetone and they were weighed by means of electrical weighing machine with 0.002 g accuracy. For elevated temperature tests (100 °C and 200 °C), the pin holding knob was tightened on to main arm and temperature was set accordingly and the procedure is repeated. Further, the surface morphology of worn samples were explored using SEM/EDS.

3. Results and discussion

3.1. SEM/EDS and XRD

Fig. 1(a) shows an SEM micrograph of 6061Al/B_4C_p composites consisting of 11 wt% of B_4C processed at 750 °C. A fairly uniform distribution of B_4C particles were observed throughout the matrix with few agglomeration at certain places. The enriched distribution is due to enhancement in the wettability that can be accredited to the inclusion of K_2TiF_6 salt. Baradeswaran and Perumal [16] detected that an addition of K_2TiF_6 flux to Al melt yields an oxide layer on the surface of Al to break and permits B_4C particles to enter the melt that subsequently advances wettability. SEM micrographs presented a compound layer adjoining the B_4C particle.

In order to portray the layer, an EDS spectrum was obtained from the boundary of the particle and is presented in Fig. 1b. The EDS spectrum have Ti, B, O, K and Al, which clearly specifies existence of Ti. A comparable Ti layer was witnessed by Toptan et al. [17] and Auradi et al. [18] round B_4C particles in their examination on preparation of Al/B_4C_p composite and determined that it consists of Ti. The Ti layer might possibly be developed due to the reaction between K_2TiF_6 - liquid Al - B_4C_p. It is assumed that K_2TiF_6 experiences an exothermic reaction upon coming into interaction with the Al melt. This reaction being vital and exothermic in nature leads to the development of an Al_3Ti-TiB_2 compound layer which might have stemmed in the increased wettability of B_4C_p. Powder XRD analysis was carried out on 6061Al/B_4C composite containing 11 wt% of B_4C particulates and presented in Fig. 1(c). XRD peaks revealed the occurrence of the major phases such as B_4C, α-Al and minor phases such as Al_3BC and Al_3Ti. Existence of Al_3Ti phase is a pure indication of the Ti compound that was formed round the B_4C particles. The reaction between Al matrix and B_4C primes to the creation of Al_3BC and AlB_2 at a temperature >868 °C. Al_3BC
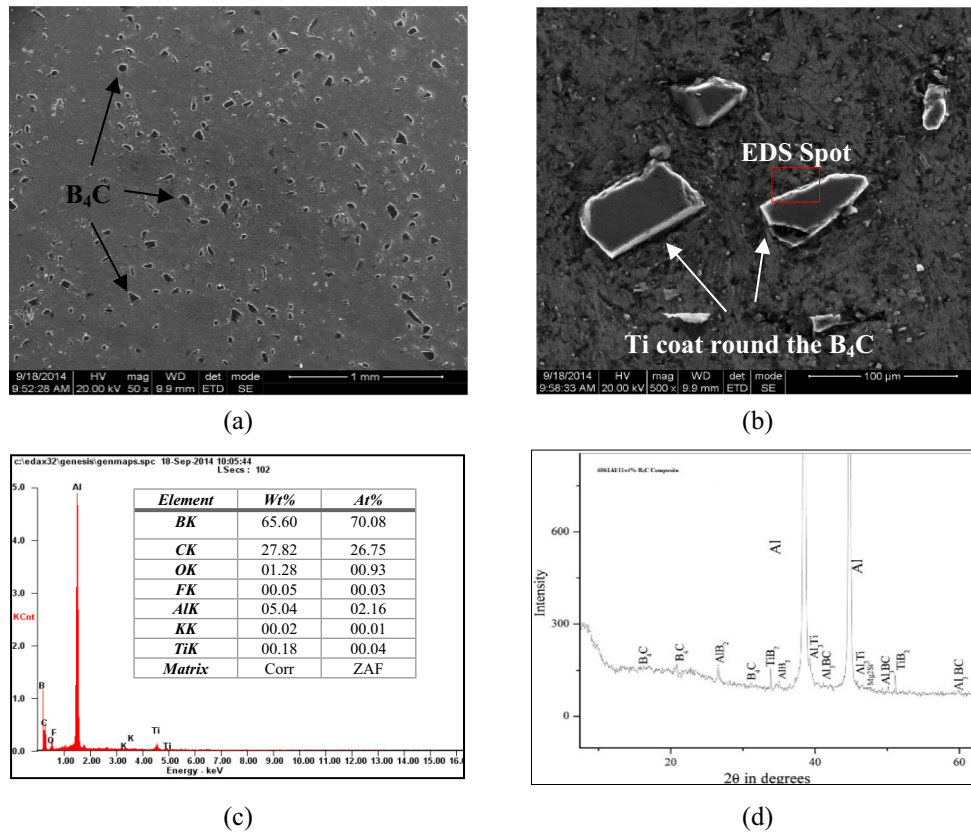
Fig. 1. (a–d). SEM micrographs shows a) dispersal of 11 wt% of B_4C_p evenly throughout the 6061Al matrix; b) appearance of white Ti coat round the B_4C_p; c) EDS pattern of the portion selected; d) XRD peaks confirming the occurrence of major and minor phase during synthesis of Al/B_4C composite.

can still be occurred while $Al_3B_{48}C_2$ substitutes AlB_2 [19–22]. Since the current work involved production of 6061Al/B_4C composites at a lower temperature 750 °C, the predictable phases would be Al_3BC and AlB_2, and only Al_3BC would be spotted. Additionally, the low concentration of Al_3BC peak proposes that not entire the B_4C particles are participated in the chemical interaction with 6061Al, perhaps the particles which are bare by the Ti coat might contribute to the creation of Al_3BC.

3.2. Overall density and micro hardness of Al/B_4C system

The density (both theoretical and experimental) and hardness (Micro Testing) of the composites are evaluated and are presented in Table 1. From Table 1 it is clear that the addition of B_4C_p to Al lowers the density and increases micro hardness of the 6061Al. Hardness of a soft material rises when hard particles combine them and it inhibits material from plastic deformation [23,24]. Grain size of material drops during solidification, as hard particles within molten metal affords extra heterogeneous nucleating locations. This results in hardness enrichment in a material. Density of prepared composite is fewer that of 6061Al matrix; B_4C has density of 2.52 g/cc. B_4C were mixed with support of flux permitting more volume of B_4C_p to blend with melt, in doing so, dropping the density of the Al/Boron carbide composite [18]. The porosity observed

could be due to features like gas trap in melt, pour timing, shrinkage, H-evaluation etc. [25,18].

3.3. Tensile strength at 100 °C and 200 °C

Normally composite materials processed at high temperatures unveil thermal residual stresses when cooled to room temperature due to variances in coefficient of thermal expansion (CTE) of the integral phases (CTE of 6061Al is 23.5×10^{-6} K and of B_4C_P is 5×10^{-6} K). According to Author Dieter [26], the established residual stresses have some adverse effects such as weakened fatigue strength, hastened stress corrosion, and shape distortion. It is clear from Table 2 that tensile strength (UTS) of 6061Al alloy has increased upon addition of 11 wt% of B_4C_p under room temperature test condition. B_4C_P acts as coherent particles through which dislocations can move, but only at stress altitudes greatly beyond the one essential to travel dislocations through the matrix phase. As a result, the second phase particles act in two discrete conducts to hinder the movement of dislocations. The particles either may be divide by the dislocations or the particles repel cutting and the dislocations are enforced to evade them. Under the applied tensile stress, huge amount of B_4C particles and the grain margins act as a hurdle to dislocation movement and result in dislocation pile ups leading to rise in the UTS of 6061Al/B_4C system. It is also

Table 1
Physical properties and micro-hardness of 6061Al alloy and it's composite.

Nominal composition	Theoretical ρ (g/cc)	Experimental ρ (g/cc)	% Error	% Porosity	Micro hardness (VHN)
6061Al	2.70	2.6740	0.9723	0.9629	72.18
6061Al-11 wt% B_4C composite	2.6872	2.6142	2.7924	3.1778	152.04

Table 2
Influence of test temperature on the UTS of 6061Al alloy and the prepared composite.

Nominal composition	Test temperature	UTS in MPa
As cast 6061Al alloy	R_t	102.56
	100 °C	97.35
	200 °C	92.06
6061Al/11 wt% B_4C Composite	R_t	136.44
	100 °C	129.82
	200 °C	118.29

Fig. 3. Wear property of 6061Al/B_4C composite under normal load ranging from 9.81 N to 39.24 N at different test temperatures respectively.

assumed that B_4C_p, when added to Al matrix act as heterogeneous nucleating spots during solidification and lead to shrinkage in grain size (coarse grain arrangement) and thus enhancement the tensile strength. At test temperature of 100 °C, the composites showed lesser ultimate tensile strength (from Table 2), which could be due to supplementary slip systems stimulated by thermal assist (Orowan looping, i.e., Orowan strengthening mechanism [27,28]).

The mechanism explains that reinforcement particulates act as pinning points of dislocations and prostration leads to unpinning, parting behind dislocation rings round the particles. The past researcher [11] witnessed that increasing temperature consents more slip systems to operate, letting general plastic deformation to happen prior to the failure. With further increase level of test temperature (200 °C), the composite shows moderate ductility; thermally assisted slips, developing large number of dislocation in Al matrix. Hence it can be concluded that Orowan strengthening had the most leading effect in reduction of tensile strength in 6061Al-11 wt% B_4C_p composite under elevated test temperature condition. Fracture surface of composite (Fig. 2a) exhibited a two-way distribution of dimples, i.e., the greater dimples were employed by the B_4C, while smaller dimples were due to ductile failure of the 6061Al under room temperature condition. Hairline cracks on B_4C_p, partial de-cohesion between matrix and reinforcement, as well as cracks in the matrix were observed. It was noticed that B_4C had fractured more than de-cohered, which means that the great interfacial strengths govern in these composites. On the other hand, medium size dimples with de-cohered B_4C; could be due to transition of brittle to severe ductile fracture under the influence of test temperature were seen and is represented in Fig. 2b and 2c. Therefore, the UTS results (Table 2) obtained is fairly acceptable and can be co-related with fractography analysis.

3.4. Effect of test temperature on the wear property of B_4C/6061Al MMC's under normal load condition

Results clearly disclose that addition of 11 wt% B_4C_p had lower the wear of Al6061 alloy at all loading condition under room temperature test. Al being poorer yield strength compared to disc material experiences severe plastic deformation while sliding;
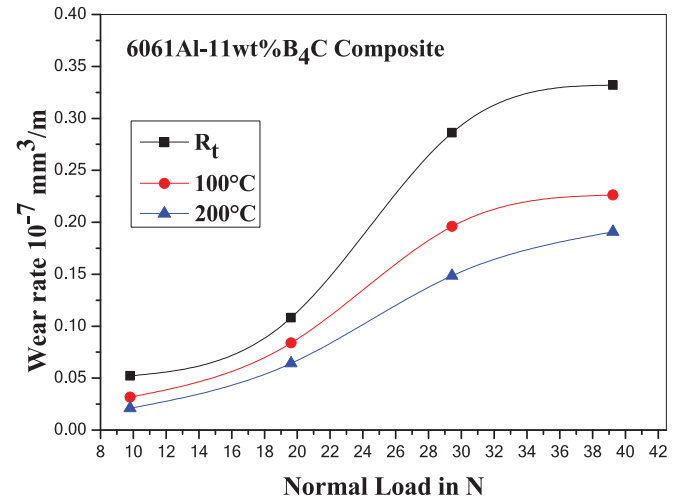
Since Al comes in interaction with steel metal, it is labelled as metal–metal contact. These metal to metal contact is disturbed by B_4C particles distributed within the Al matrix resulting in 2 body abrasion mechanism. A layer comprising of oxides, counter surface material, pull out particles and wear debris at the interface termed as mechanically mixed layer (MML); causes strain hardening in 6061Al matrix which decrease the wear rate of composite under all normal loads as evident from Fig. 3. Similar outcome was observed by Uyyuru et al. [29] and Uthayakumar et al. [13] in their work. Worn micrographs of cast composite (Fig. 4a) showed narrow grooves along the sliding direction, few scratches at certain area and clustered white fragments. Such topographies are features of abrasion, where asperities of the steel disc or hard reinforced particles in between the contacting faces, plough or cut into the pin, causing wear by the removal of small fragments from the worn surface. The white compact surfaces are characteristics of oxidative wear, in which frictional heating while sliding sources oxidation of the surface, with wear taking place through the elimination of oxide fragments as wear debris.

The concept of thermal softening can be employed here in order to discuss the reason for increased wear rate under high temperature test condition. At 100 °C testing, the frictional force between the pin and disc combines with set temperature that stimulates plastic deformation in spite of B_4C particle leading to severe wear loss at all loading condition, as evident from Fig. 3. Further, with additional level of temperature, MML diminishes gradually and delamination of wear surface occurs which decreases the wear rate of composite. It is believed that under high load, the contact pres-
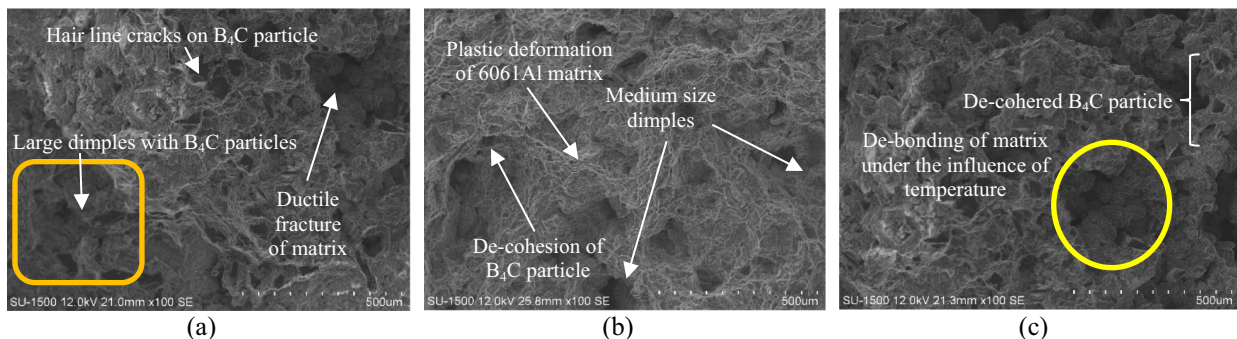

Fig. 2. (a–c). SEM micrographs of 6061Al/11 wt% B_4C composite fractured by the tensile stress under different test temperatures a) Room temperature; b) 100 °C; c) 200 °C.
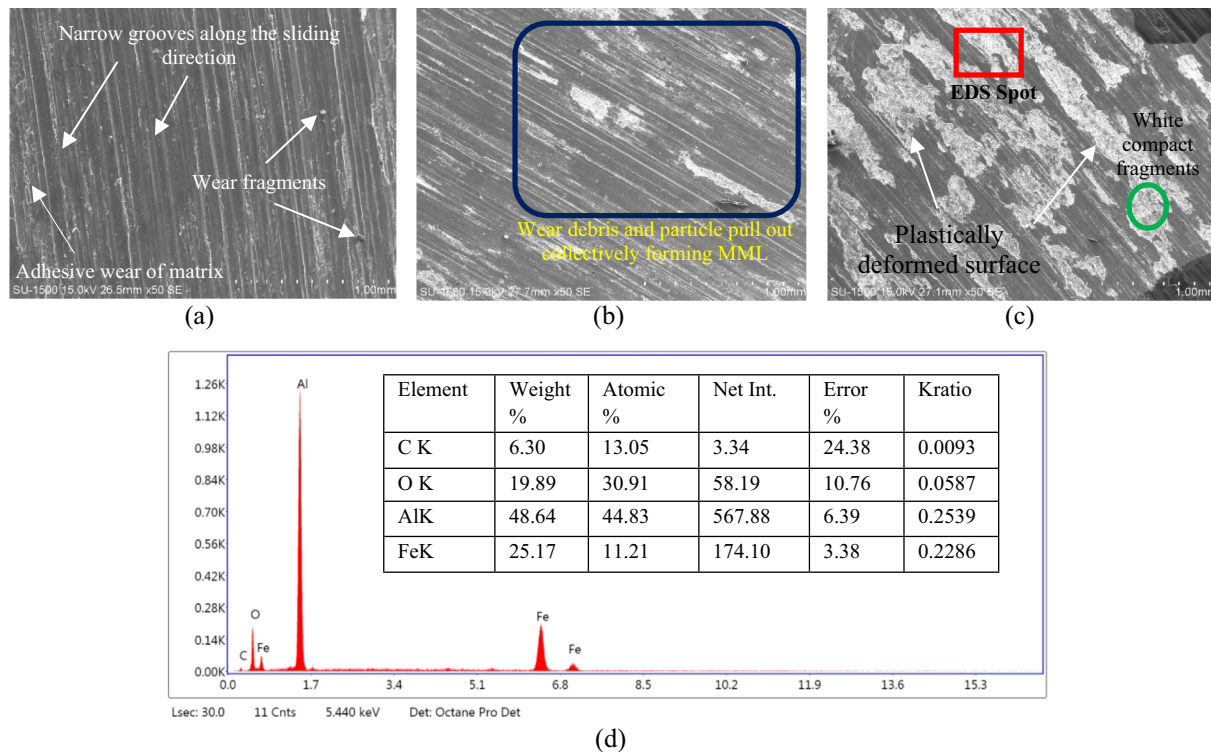
Fig. 4. (a–d). Worn surface micrographs of 6061Al/11wt.%B$_4$C composite tested under 39.24 N applied load for sliding distance of 500 m with sliding velocity of 1.879 m/s at test temperature a) Rt; b) 100 °C; c) 200 °C; d) EDS taken at the marked area.

sure at the Pin-Disc interface and thermal softening in presence of test temperature together forces MML to wear out rapidly ensuing more wear loss of 6061Al/B$_4$C composite.

Mixture of small and medium size grooves along the sliding direction, plastically deformed surface and agglomerated wear debris were observed (Fig. 4b and 4c) which specifies abrasive to adhesion type wear mechanism under the influence of test temperature at all load condition. Existence of "O" and "Fe" peak in the EDS pattern (Fig. 4d) confirms the oxidation layer and micro ploughing on steel disc at higher test temperature. Hence, temperature plays a vital role in the property evaluation of B$_4$C reinforced 6061Al metal matrix composites.

4. Conclusion

In the present study, the tensile strength (UTS) and sliding wear properties of 6061Al/11 wt% B$_4$C composite were evaluated under different test temperatures i.e. 100 °C and 200 °C. Introduction of K$_2$TiF$_6$ along with B$_4$C particles in the ratio of 0.2 has supported in advancing wettability of the B$_4$C particle by the 6061Al matrix at 750 °C, which is clear from SEM micrographs. Density of composite material was found lower (2.6142 g/cc) compared to cast Al alloy. Hardness of 6061Al matrix alloy has improved from 72.18 VHN to 152.04 VHN by addition of B$_4$C$_p$. Grain size of material drops during solidification, as hard particles within molten metal affords extra heterogeneous nucleating locations resulting in enrichment in material hardness. The tensile strength (UTS) of 6061Al alloy has increased upon addition of 11 wt% of B$_4$C$_p$ under the room temperature test condition. Under the applied tensile stress, huge amount of B$_4$C particles and the grain margins act as a hurdle to dislocation movement and result in dislocation pile ups leading to rise in the UTS of 6061Al/B$_4$C system. At test temperature of 100 °C and 200 °C, the composites showed lesser ultimate tensile strength which could be due to supplementary slip systems stimulated by thermal assist; Orowan strengthening. Hence it can be decided that Orowan strengthening had the most leading effect in the reduction of tensile strength in 6061Al-11 wt% B$_4$C$_p$ composite under high test temperature condition and was evident from fractography micrographs. Wear results clearly shows that addition of 11 wt% B$_4$C$_p$ had lower the wear of Al6061 alloy at all loading condition under room temperature test. At 100 °C testing, the frictional force between the pin and disc combines with set temperature that stimulates plastic deformation (overcomes MML shield) in spite of B$_4$C particle leading to severe wear loss. Further, with additional level of temperature, mechanically mixed layer diminishes gradually and delamination of wear surface occurs which decreases the wear rate of composite. Mixture of small and medium size grooves along the sliding direction, plastically deformed surface and agglomerated wear debris was observed from worn surface SEM micrographs which specifies abrasive to adhesion type wear under the influence of test temperature at all load condition. Presence of "O" and "Fe" peak in the EDS pattern (EDS taken on the worn surface) confirms the oxidation layer formation and micro ploughing on steel disc at elevated test temperature.

Declaration of Competing Interest

The authors declare that they have no known competing financial interests or personal relationships that could have appeared to influence the work reported in this paper.

Acknowledgements

References

[1] M. Aizenshtein, N. Froumin, T.E. Shapiro, M.P. Dariel, N. Frage, Scr. Mater. 53 (2005) 1231–1235.
[2] J. Jung, S. Kang, J. Am. Ceram. Soc. 87 (1) (2004) 47–54.
[3] K.B. Lee, H.S. Sim, S.H. Kim, K.H. Han, H. Kwon, J. Mater. Sci. 36 (13) (2001) 3179–3188.
[4] D.C. Halverson, A.J. Pyzik, I.A. Aksay, W.E. Snowden, J. Am. Ceram. Soc. 72 (5) (1989) 775–780.
[5] A.R. Kennedy, B. Brampton, Sci. Mater. 44 (2001) 1077–1082.
[6] J.J. Lewandowski, C. Liu, W.H. Hunt Jr, Mater. Sci. Eng. A. 107 (1989) 241–255.
[7] K.B. Lee, H.S. Sim, S.Y. Cho, H. Kwon, Metall. Mater. Trans. A. 32A (2001) 2142–2147.
[8] P.M. Singh, J.J. Lewandowski, Metall. Mater. Trans. A. 24A (1993) 2531–2543.
[9] Y. Flom, R.J. Arsenault, Acta Metall. 37 (9) (1989) 2413–2423.
[10] S. Ho, E.J. Lavernia, Appl. Compos. Mater. 2 (1995) 1–30.
[11] A.M. Maniatty, D.J. Littlewood, J. Lu, J. Eng. Mater. Technol. 130 (2008) 1–9, 021019.
[12] B.C. Majumdar, Introduction to Tribology of Bearings, first ed., A. H. Wheeler & co. Pvt ltd, Allahabad India, 1986.
[13] M. Uthayakumar, S. Aravindan, K. Rajkumar, Mater. Des. 47 (2013) 456–464.
[14] I. Kerti, F. Toptan, Mater. Lett. 62 (8) (2008) 1215–1218.
[15] W. Zhou, Z.M. Xu, J. Mater. Process. Technol. 63 (1–3) (1997) 358–363.
[16] A. Baradeswaran, A. Elaya Perumal, Composites Part B. 54 (2013) 146–152.
[17] F. Toptan, A. Kilicarslan, A. Karaaslan, M. Cigdem, I. Kerti, Mater. Des. 31 (2010) S87–S91.
[18] V. Auradi, G.L. Rajesh, S.A. Kori, Procedia Mater. Sci. 6 (2014) 1068–1076.
[19] H.M. Hu, E.J. Lavernia, W.C. Harrigan, J. Kajuch, S.R. Nutt, Mater. Sci. Eng., A. 297 (2001) 94–104.
[20] K.B. Lee, H.S. Sim, S.Y. Cho, H. Kwon, Mater. Sci. Eng. A. 302 (2001) 227–234.
[21] J.P. Lucas, J.J. Stephens, F.A. Greulich, Mater. Sci. Eng. A. 131 (2) (1991) 221–230.
[22] J. Kellie, J.V. Wood, Mater. World. 3 (1995) 10–14.
[23] C.S. Ramesh, R. Keshavamurthy, B.H. Channabasappa, Abrar Ahmed, Mater. Sci. Eng. A. 502 (1–2) (2009) 99–106.
[24] G.L. Rajesh, V. Auradi, S.A. Kori Umashankar, Procedia Mater. Sci. 5 (2014) 289–294.
[25] J. Hasim, L. Looney, M.S.J. Hashmi, J. Mater. Process. Technol. 92–93 (1999) 1–7.
[26] G.E. Dieter, Mechanical Metallurgy, third ed., McGraw-Hill, Berlin, 1986.
[27] S. Queyreau, G. Monnet, B. Devincre, Acta Mater. 58 (17) (2010) 5586–5595.
[28] B.G. Park, A.G. Crosky, A.K. Hellier, Composites Part B. 39 (7–8) (2008) 1257–1269.
[29] R.K. Uyyuru, M.K. Surappa, S. Brusethaug, Wear. 260 (11–12) (2006) 1248–1255.

Cost-Effective Spectrum Utilization for Futuristic Cognitive Radio based Services

Chanda V. Reddy

Abstract: *The proliferation of various mobile users in the context of advanced wireless technologies, spectrum scarcity arises as a crucial problem. The notion of cognitive radio (CR) principle offers cost-effective spectrum reusability with intelligent mode of transmission model. It basically enables a radio-driven technology to utilize dynamic spectrum accessing to meet the quality-of-services (QoS) requirements by satisfying enormous communication and connectivity demands. To alleviate the spectrum scarcity problem the study proposes a novel analytical solution of spectrum allocation considering a simplified evolutionary learning model. The prime target of the formulated concept is to detects the spectrum holes effectively for reusability and the possibility of identification has be maximized for best possible spectrum allocation to the radios. And on the other hand also the occurrence of false positive identification has to be minimized. The outcome obtained after performing the simulation shows promising aspects in the context of effective spectrum· allocation for higher priority user with better throughput performance.*

Keywords: *Cognitive Radio, Spectrum Allocation, multi-objective optimization, Throughput performance*

I. INTRODUCTION

In the recent scenario researchers from IEEE and many other communication societies are more concerned towards improving the communication paradigm in the context of 5G wireless technologies. The underlying principle of cognitive radio (CR) technology opens up a new opportunity for effective spectrum utilization and also aroused significant attention for its wider prospects [1] [2]. CR has been introduced to tackle the issue connected with the constraints of bandwidth availability of conventional wireless communication standards which is tightly licensed and restricted by the Government policies. Thereby, it can be seen that mobile devise are restricted to utilize a certain value of frequency and hence a bottle-neck scenario arises in reality due to limited bandwidth where the number of mobile users are tremendously increasing. Thereby maintain quality of service aspects (QoS) with effective spectrum utilization has become crucial. CR technology can easily handle this issue of spectral scarcity by meeting the growing demand of mobile user requirements and also has become a reliable solution to solve the spectral congestion problem in the modern wireless communication [3][4]. CR is utilized as an extended technology component of software defined radio (SDR) and also incorporates an intelligent system of sensing and channel management functionality. There exist various time-critical applications of CR such as into public safety networks,

disaster relief and emergency networks etc. and it is highly agile for advanced intelligent communication systems considering its autonomous mode of selection of operating parameters [5][6]. The figure 1 presents and overview of the advanced paradigm in CR based radio communications.
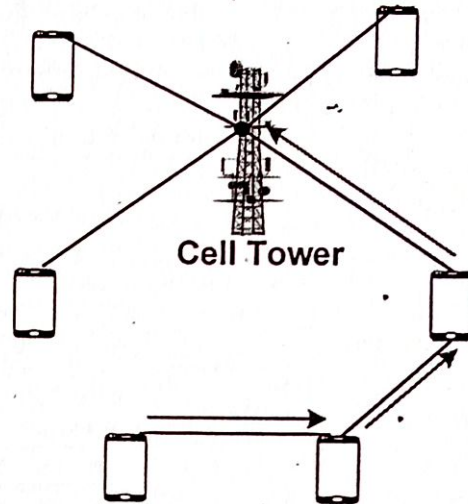

Fig 1 Radio communication in CR

Fig.1 shows that how the CR enabled communication facilitates mobile devices to communicate with each other so that communication between a mobile client and cell-tower can be established with higher throughput efficiency [7][8]. This research study addresses the spectrum allocation problem in the modern wireless communication technology and aims to formulate an energy efficient optimized transmission model based on CR to attain better end-to-end throughput performance. The system modeling of CR is designed with an objective to perform intelligent resource scheduling in variable traffic conditions in the context of advanced cellular networking operations. For this purpose the methodology aims to maximize the spectrum utilization performance considering a metaheuristics evolutionary learning model with lower complexity to attain best possible outcome. The entire manuscript is presented with respect to different sections, *section II* highlights the existing trend of research based studies on CR and outlines the gap in reality. *Section III* finally extracts the cumulative research problem which is jointly addressed in this study with problem formulation aspect.

Finally section IV highlights a comprehensive discussion on proposed analytical system design for CR assisted effective spectrum resource management.

The mathematical modeling is formulated for best possible available spectrum allocation to the SDR with higher possibility of available spectrum detection and also· minimizing

Retrieval Number: D1616029420·2020©BEIESP
DOI: 10.35940/ijitee.D1616.029420

2476

Published By:
Blue Eyes Intelligence Engineering
& Sciences Publication

☐   4010

A novel and integrated architecture for identification and cancellation of noise from GSM signal

Rekha N[1], Fathima Jabeen[2]
[1]Department of Electronics and Communication Engineering, K.S. Institute of Technology, India
[2]Islamiah Institute of Technology, India

Article Info	ABSTRACT
	There are multiple reasons for the evolution as well as the presence of noise over transmitted GSM signal. In spite of various approaches towards noise cancellation techniques, there are less applicable techniques for controlling noise in acoustic GSM signal. Therefore, the proposed manuscript presents an integrated modelling which performs modelling of noise identification that could significantly assist in successful noise cancellation. The proposed system uses three different approach viz. i) stochastic based approach for noise modelling, ii) analytical-based approach where allocated power acts as one of the prominent factors of noise, and iii) wavelet-based approach for effective decomposition of GSM signal for assisting better noise cancellation technique followed by better retention of signal quality. Simulated in MATLAB, the study outcome shows that it offers a cost-effective implementation, A Practical Approach for Noise identification, and Effective Noise Cancellation with Signal quality retention. The proposed system offers approximately 24% of enhancement in noise reduction as compared to any existing digital filters with 1.6 seconds faster in processing speed.

Corresponding Author:

Rekha N,
Research Scholar, Department of Electronics and Communication Engineering,
K.S. Institute of Technology, Bengaluru, India.
Email: rekhaphd2014@gmail.com

1. INTRODUCTION

Since last few years, the GSM-based wireless communication has been accounted for emerging growth in the telecom industries. The GSM was introduced as a progression of second-generation cellular technology specified with digital modulation service. At present, the development of the GSM standard has reached the level of meeting daily needs of users and enterprises by providing cost-effective voice services as well as efficient data services which can be accessed 24x7 irrespective of user's location [1]. GSM technology supports various features for its global acceptance and rich popularity [2]. Such features are like it has efficient spectrum, good voice quality service supports low-cost cellular devices, compatible with ISDN and new services and provides roaming services globally. With the evolution of GSM, there are many advances made in digital devices, such as personal digital assistants, PCs, mobile phones, wireless LANs, etc [3]. These devices are enabled with the support of cellular communication module in order to deliver on-demand services and entertainment in various fields of application such as schools, office, healthcare, transport, Industrial area, and many more [4].

In a cellular communication system, the speech and data information transmitted via a radio link communication channel where the quality of transmitted data suffers from many degradation factors such as background noise and channel interferences [5]. The 'term' noise and interference basically refers to unwanted destructive signals introduced into use-full speech and data signals. The sources of noise are varied in nature it can be generated from an environmental factor such as acoustic disturbance form traffic, blowing

Implementing and analysing FAR and FRR for face and voice recognition (multimodal) using KNN classifier

Dinesh Kumar D.S.

TJIT, Visvesvaraya Technological University, Belagavi, India and
KSIT, Bangalore, India, and

P.V. Rao

TJIT, Bangalore, India and
VBIT, Hyderabad, India

Abstract

Purpose – The purpose of this paper is to incorporate a multimodal biometric system, which plays a major role in improving the accuracy and reducing FAR and FRR performance metrics. Biometrics plays a major role in several areas including military applications because of robustness of the system. Speech and face data are considered as key elements that are commonly used for multimodal biometric applications, as they are simultaneously acquired from camera and microphone.

Design/methodology/approach – In this proposed work, Viola–Jones algorithm is used for face detection, and Local Binary Pattern consists of texture operators that perform thresholding operation to extract the features of face. Mel-frequency cepstral coefficients exploit the performances of voice data, and median filter is used for removing noise. KNN classifier is used for fusion of both face and voice. The proposed method produces better results in noisy environment with better accuracy. In this proposed method, from the database, 120 face and voice samples are trained and tested with simulation results using MATLAB tool that improves performance in better recognition and accuracy.

Findings – The algorithms perform better for both face and voice recognition. The outcome of this work provides better accuracy up to 98 per cent with reduced FAR of 0.5 per cent and FRR of 0.75 per cent.

Originality/value – The algorithms perform better for both face and voice recognition. The outcome of this work provides better accuracy up to 98 per cent with reduced FAR of 0.5 per cent and FRR of 0.75 per cent.

Keywords FAR, LBP, MFCC, DCT, KNN

Paper type Research paper

1. Introduction

In the modern world, biometrics is used to authenticate and identify a person. Biometrics combines the physical traits and behavioural characteristics for identity verification. It provides a suitable solution to our security needs with better accuracy. A person can be identified accurately using biometrics based on unique physical or behavioural characteristics. Multimodal biometric authentication is widely used in banking security, credit card transactions and passport verification combining different biometric traits.

1.1 Problem statement

Biometrics is widely used for authentication and identification of a person based on physiological and behavioural traits such as face, iris, palm print, signature, etc. There are several drawbacks of unimodal biometric systems such as intra-class variation, inter-class

Power-Cognizant Proactive Routing Protocol for Amending Energy in Ad-hoc Networks

B. Devika[✉] and P. N. Sudha

KSIT, Bengaluru, India
{devikabgowda, pnsudha}@gmail.com

Abstract. The execution of an Ad hoc Wireless Network is controlled by a key factor "power", as it is the essential resource of any communication system. Utilizing such power effectively and efficiently is the most important Task. Power has to be optimized according to the requirement. In an ad hoc network, nodes exchange information with each other by forming a multi-hop wireless network & sustaining connectivity in a localized fashion. Optimizing power in such a network is a significant challenge ad hoc routing protocols are power hungry as they expend a substantially large amount of battery power contained in the nodes. Hence routing in an ad hoc network is eminently power restricted. Research has been done choosing the appropriate routing protocol at the network layer and power aware protocol at MAC layer. In this paper, a proactive routing protocol has been implemented which is power aware. FSR is the routing protocol chosen and MAC 802.11 standards have been used in combination of a routing protocol to optimize power. The simulation is executed using NS-2 and the power consumption has reduced.

Keywords: Ad hoc networks · Fisheye state · Manet · Mac · Power cognizant

1 Introduction

Wireless communication is the quickly expanding & most vital technological areas in the communication field. Our lives are unimaginable without Wireless communication like TV, Radio, Mobile, Radar, GPS, Wifi, Bluetooth, RFID etc. In Latin ad hoc means "for this purpose". Ad hoc networks are group of self-organizing nodes or terminals that exchange information with each other by combining a multi-hop wireless network and sustaining connectivity in a suburbanized manner in an infrastructure less environment. Several classifications of Ad hoc networks are MANET, VANET, FANET, WSN etc. Ad hoc network operate with IEEE 802-11 standards. Initially ad hoc networks were designed for military and disaster recovery applications, due to their fast deployment feature without the existence of any infrastructure. But with rapid growth of mobile communication, MANETs are regarded as important contemplate in the future inception of system technologies [1].

Various power optimization techniques are existent in Ad hoc networks. Optimization of power is of at most importance in Ad hoc networks as their structure is autonomous and non-existence of central governing body. Various layers are affected while optimizing power in ad hoc network like physical, network & MAC layer [2].

A COMPARATIVE ANALYSIS OF DES AND BAES FOR MANET

Srividya R

K. S. Institute of Technology, Bangalore, Karnataka, India

Ramesh B

Department of Computer Science and Engineering,
MCE - Malnad College of Engineering, Hassan, Karnataka, India

ABSTRACT

The exponential increase in digital data exchange in Mobile Ad hoc network paves a way for authentic research in the horizon of securing data using cryptographic methods. This paper proposes a comparative analysis of existing DES and proposed Biometric Advanced Encryption Standard (BAES) cryptographic algorithm. BAES implementation includes design of robust biometric key generation algorithm that can mitigate malicious attacks by extending security definitions of existing Advanced Encryption Standard.

Key words: MANET, BAES, DES, Fingerprint, Minutiae.

1. INTRODUCTION

Mobile Ad hoc Network (MANET) is known for its self configuring and dynamic nature and its capability to exchange data between mobile nodes. Due to MANET's dynamic nature, providing secure data mobility is a challenging task. Passive or active attacks can be launched effortlessly in such networks with no centralized management and firewall. To secure the data from being permuted or eavesdropped is a confronting assignment. It is intricate to detect passive attacks like eavesdropping. Hence the outstanding schema would be to use a cryptographic method and encrypt the data before transmitting it into MANET. The past few decades have seen an exponential rise in the genre of cryptographic algorithm innovations and inventions. The study of literature illustrates ample of encryption algorithms and their applications. Here we propose and develop a cryptographic method Biometric Advanced Encryption Standard (BAES), which is a petty contribution to the sphere of cryptographic algorithms. An effort is put in, to compare BAES with Data Encryption Standard (DES) considering time and memory parameters.

◻   4266

Implementation of AES using biometric

Srividya R[1], Ramesh B[2]
[1]Department of Telecommunication Engineering, K.S. Institute of Technology, India
[2]Department of Computer Science and Engineering, Malnad College of Engineering, India

Article Info	ABSTRACT
	Mobile Adhoc network is the most advanced emerging technology in the field of wireless communication. MANETs mainly have the capacity of self-forming, self-healing, enabling peer to peer communication between the nodes, without relying on any centralized network architecture. MANETs are made applicable mainly to military applications, rescue operations and home networking. Practically, MANET could be attacked by several ways using multiple methods. Research on MANET emphasizes on data security issues, as the Adhoc network does not befit security mechanism associated with static networks. This paper focuses mainly on data security techniques incorporated in MANET. Also this paper proposes an implementation of Advanced Encryption Standard using biometric key for MANETs. AES implementation includes, the design of most robust Substitution-Box implementation which defines a nonlinear behavior and mitigates malicious attacks, with an extended security definition. The key for AES is generated using most reliable, robust and precise biometric processing. In this paper, the input message is encrypted by AES powered by secured nonlinear S-box using finger print biometric feature and is decrypted using the reverse process.

Corresponding Author:

Srividya R,
Department of Telecommunication Engineering,
K.S. Institute of Technology,
#14, Raghuvanahalli, Kanakapura main road, Bangalore-109, India.
Email: srividya.ramisetty@gmail.com

1.   INTRODUCTION

MANET is a wireless Adhoc Network which is dynamic in nature. It has the capability to transmit signals in between mobile nodes. Its self-configuration property essentially deals with dynamic property of moving nodes. MANET does not have organized network infrastructure in order to establish communication, because of its agility. This imposes limitations on network infrastructure, data security, processing ability, throughput and performance of the system [1]. Data security for MANET is to be designed keeping processing power and speed into consideration. Hence the deployment environment defines an extensive security at the cost of low processing power and at high data rate. MANET has on-demand need for high level security systems incorporated in network infrastructure. The literature stream lines wide number of security systems applicable to network systems. Most popular Cryptographic system illustrated in literature is advanced encryption system (AES). AES is distinguished encryption and decryption system used widely in vital computer networking applications. Key generation used to encrypt input message is again a very important aspect in data encryption/decryption systems. Use of symmetric key and asymmetric key remarks its own merits and demerits in securing data and data mobility in MANETs.

Main motivation behind data security in context of MANET is not only to secure data at high speed, but also at reduced processing power. Hence the usage of key generation is limited to implementation of symmetric key generation. However symmetric key generation is also made complex by generating the key

COMPUTATIONAL ANALYSIS OF MICRO CHANNEL PATH OPTIMIZATION OF HEAT EXCHANGER BASED ON THERMAL BOUNDARY CONCEPT

Jalaja.P[1], Shivakumar H.M[2]

[1] Department of Mathematics, K.S.Institute of Technology, Bangalore – 560109

[2] Department of Mathematics , East West Institute of Technology, Bangalore – 560 091

[1] pjmaths@gmail.com

[2] hmsk78@gmail.com

ABSTRACT

This paper deals with the optimization of channel profile of printed circuit heat exchangers for the turbulent flow regime. The properties of the inner and outer wall of each channel have been studied as these are the regions that participate in the heat transfer. Numerous investigations exist that deal with the heat transfer characteristics for zig-zag channels of varying angles and pitch length but do not explicitly indicate the performance variations in the regions of the bend and interacting walls. Existing studies for channel profile optimization of printed circuit heat exchanger deal with the laminar flow regime. This study precisely expresses the elevation of heat transfer coefficient in the regions of the bend coupled with a rise in the pressure drop. CFD study is done to optimize the effectiveness of the heat exchanger; used as a recuperator/intermediate HX in S-CO2 Brayton cycle test loop. 3D steady state simulations on commercial CFD code FLUENT using the k-ε realizable model with standard wall function and coupled boundary wall is implemented. The working fluid in this investigation is Supercritical CO-2, water and Alloy 617 as a solid substrate. For fixed inlet conditions the heat transfer coefficient is studied in the flow domain by maintaining constant pitch length and different channel angle (60°- 180°). The second study incorporates an investigation by keeping the θ constant and varying the pitch length(20 mm- 40 mm). This analysis compares the effect of the heat transfer characteristics of a fully developed flow to a developing flow. Channels with lower θ give rise to better heat transfer characteristics at the cost of elevation of pressure drop, while a fully developed flow has lower heat transfer characteristics compared to a developing flow for a fluid losing heat. A comprehensive study indicating the thermal-hydraulic properties at various regions in the 3D wavy PCHE for the turbulent region is presented here.

1. Introduction

The use of S-CO2 in Brayton cycle test loop has received tremendous attention as a promising technology to replace the water-based Rankine cycle. One of the key features of the S-CO2 Brayton cycle loop is that a significant portion of the heat(60-70%) is regenerated after the turbine exhaust[1]. Therefore the exhaust gas recovery system must be efficient and capture a substantial portion of the residual heat. Component level